

Chapter 5

Particles and Symmetries



Symmetry simplifies the description of physical phenomena, in such a way that humans can understand them: the Latin word for “understanding,” capere, also means “to contain”; and as we are a part of it we cannot contain the full Universe, unless we find a way to reduce its complexity—this is the meaning of symmetry. Symmetry plays a particularly important role in particle physics, as it does in astrophysics and in cosmology. The key mathematical framework for symmetry is group theory: symmetry transformations form groups. Although the symmetries of a physical system are not sufficient to fully describe its behavior—for this purpose, one needs a complete dynamical theory—it is possible to use symmetry to discover fundamental properties of a system. Examples of symmetries include space–time symmetries, internal symmetries of particles, and the so-called gauge symmetries of field theories.

5.1 A Zoo of Particles

In the beginning of the 1930s, just a few particles were known: the proton and the electron, the charged constituents of the atom; the neutron, which was ensuring the stability of the atomic nuclei; the neutrino (predicted but by then not discovered yet), whose existence was conjectured to guarantee the conservation of energy and momentum in beta decays; and the photon, i.e., the quantum of the electromagnetic field. Then, as we discussed in Chap. 3, new and often unexpected particles were discovered in cosmic rays: the positron, the antiparticle of the electron; the muon, the heavy brother of the electron; the charged pion, identified as the particle postulated by Yukawa as the mediator of the strong interaction; the strange “V” particles K^0 and Λ (called “V” from the topology of their decays in bubble chambers).

Human-made accelerators were meanwhile developed (the first linear accelerator by R. Wideroe in 1928; the first Van de Graaf by R.J. Van de Graaf in 1929; the first cyclotron by E.O. Lawrence in 1929; the first multistage voltage multiplier by J.D. Cockcroft and E.T.S. Walton in 1932). The impressive exponential increase of the energy of the beams produced by accelerators, from a few hundred keV in the 1930s

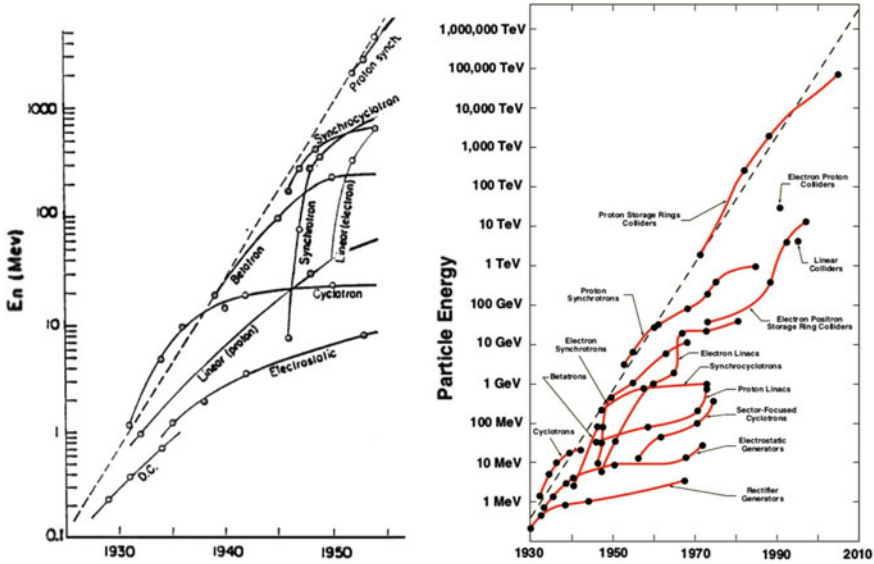


Fig. 5.1 Livingston plot, representing the maximum energies attained by accelerators as a function of the year: original (left) and updated (right). For colliders, energies are translated into the laboratory system. Original figures from M.S. Livingston and J.P. Blewett, “Particle Accelerators,” MacGraw Hill 1962; A. Chao et al. “2001 Snowmass Accelerator R&D Report,” eConf C010630 (2001) MT100

to the GeV in the beginning of the 1950s, was summarized by M. Stanley Livingston in 1954, in the so-called *Livingston plot* (Fig. 5.1). This increase went on along the last fifty years of the twentieth century, and just in the most recent years it may have reached a limit ~ 14 TeV with the Large Hadron Collider (LHC) at CERN.

Accelerators provide the possibility to explore in a systematic way the energy scale up to a few TeV, and thanks to this a huge number of new particles have been discovered. Already in the 1950s, many discoveries of particles with different masses, spins, charges, properties took place. Their names almost exhausted the Greek alphabet: these particles were called π , ρ , η , η' , ϕ , ω , Δ , Λ , Σ , Ξ . . .

Classifications had to be devised to put an order in such a complex zoology. Particles were first classified according to their masses in classes with names inspired, once again, to Greek words: heavy particles like the proton were called *baryons*; light particles like the electron were called *leptons*; and particles with intermediate masses were called *mesons*. The strict meaning of the class names was soon lost, and now we know a lepton, the tau, heavier than the proton. According to the present definition, leptons are those fermions (particles with half-integer spins) that do not interact strongly with the nuclei of atoms, while baryons are the fermions that do. Mesons are bosons (particles with integer spins) subject to strong interactions. Baryons and mesons interact thus mainly via the strong nuclear force and have a common designation of *hadrons*.

The detailed study of these particles shows that there are several conserved quantities in their interactions and decays. The total electric charge, for example, is always conserved, but also the total number of baryons appears to be conserved, and thus, the proton, being the lightest baryon, cannot decay (the present experimental limit for the proton lifetime is of about 10^{34} years). Strange particles if they decay by strong interactions give always birth to a lighter strange particle, but the same is not true when they decay via weak interactions. To each (totally or partially) conserved quantity, a new quantum number was associated: baryons, for instance, have “baryonic quantum number” $+1$ (antibaryons have baryonic quantum number -1 , and mesons have baryonic quantum number 0).

As a consequence of baryon number conservation, for example, the most economic way to produce an antiproton in a proton–proton collision is the reaction $pp \rightarrow ppp\bar{p}$. A proton beam with energy above the corresponding kinematic threshold is needed to make this process possible. The Bevatron, a proton synchrotron at the Lawrence Berkeley National Laboratory providing beams with energy of 6.2 GeV , was designed for this purpose and started operation in 1954. In the following year, Chamberlain, Segrè, Wiegand, and Ypsilantis announced the discovery of the antiproton; the new particle was identified by measuring its momentum and mass using a spectrometer with a known magnetic field, a Cherenkov detector, and a time-of-flight system. This discovery confirmed that indeed, as predicted by the Dirac equation, to each particle corresponds an oppositely charged particle with the same mass and spin.

The existence of particles and antiparticles is an example of symmetry, and symmetries became more and more present in the characterization of particles and of their interactions. Particle physicists had to study or reinvent group theory in order to profit of the possible simplifications guaranteed by the existence of symmetries.

5.2 Symmetries and Conservation Laws: The Noether Theorem

Being a part of the Universe, it is difficult to imagine how humans can expect to understand it. But we can simplify the representation of the Universe if we find that its description is symmetrical with respect to some transformations. For example, if the representation of the physical world is invariant with respect to translation in space, we can say that the laws of physics are the same everywhere, and this fact greatly simplifies our description of Nature.

The dynamical description of a system of particles can be classically expressed by the positions \mathbf{q}_j of the particles themselves, by their momenta \mathbf{p}_j and by the potentials of the interactions within the system. One way to express this is to use the so-called Hamiltonian function

$$H = K + V \tag{5.1}$$

which represents the total energy of the system (K is the term corresponding to the kinetic energies, while V corresponds to the potentials). An equivalent description, using the Lagrangian function, will be discussed in the next chapter.

From the Hamiltonian, the time evolution of the system is obtained by the Hamilton's equations:

$$\frac{dp_j}{dt} = -\frac{\partial H}{\partial q_j}; \quad \frac{dq_j}{dt} = \frac{\partial H}{\partial p_j} \quad (5.2)$$

where

$$p_j = \frac{\partial H}{\partial \dot{q}_j}. \quad (5.3)$$

For example, in the case of a single particle in a conservative field in one dimension,

$$H = \frac{p^2}{2m} + V \quad (5.4)$$

and Hamilton's equations become

$$\frac{dp}{dt} = -\frac{dV}{dx} = F; \quad \frac{dx}{dt} = \frac{p}{m}. \quad (5.5)$$

To the Hamiltonian, there corresponds a quantum mechanical operator, which in the nonrelativistic theory can be written as

$$\hat{H} = \frac{\hat{p}^2}{2m} + V. \quad (5.6)$$

We shall expand this concept in this chapter and in the next one.

Symmetries of a Hamiltonian with respect to given operations entail conservation laws: this fact is demonstrated by the famous Noether theorem.¹ In the opinion of the authors, this is one of the most elegant theorems in physics.

Let us consider an invariance of the Hamiltonian with respect to a certain transformation—for example, a translation along x . One can write

$$0 = dH = dx \frac{\partial H}{\partial x} = -dx \frac{dp_x}{dt} \implies \frac{dp_x}{dt} = 0. \quad (5.7)$$

¹Emmy Noether (1882–1935) was a German mathematician. After dismissing her original plan to become a teacher in foreign languages, she studied mathematics at the University of Erlangen, where her father was a professor. After graduating in 1907, she worked for seven years as an unpaid assistant (at the time women could not apply for academic positions). In 1915, she joined the University of Göttingen, thanks to an invitation by David Hilbert and Felix Klein, but the faculty did not allow her to receive a salary, and she worked four years unpaid. In that time, she published her famous theorem. Finally, Noether moved to the USA to take up a college professorship in Philadelphia, where she died at the age of 53.

If the Hamiltonian is invariant with respect to a translation along a coordinate, the momentum associated to this coordinate is constant. And the Hamiltonian of the world should be invariant with respect to translations if the laws of physics are the same everywhere. In a similar way, we could demonstrate that the invariance of an Hamiltonian with respect to time entails energy conservation, and the rotational invariance entails the conservation of angular momentum. These are particular cases of Noether's theorem, which will be discussed in Sect. 5.3.1.

5.3 Symmetries and Groups

A set $\{a, b, c, \dots\}$, finite or infinite, of objects or transformations (called hereafter elements of the group) form a group \mathcal{G} if there is an operation (called hereafter product and represented by the symbol \odot) between any two of its elements such that

1. It is closed: the product of any of two elements a, b is an element c of the group

$$c = a \odot b. \quad (5.8)$$

2. There is one and only one identity element: the product of any element a by the identity element e is the proper element a

$$a = a \odot e = e \odot a. \quad (5.9)$$

3. Each element has an inverse: the product of an element a by its inverse element b (designated also as a^{-1}) is the identity e

$$e = a \odot b = b \odot a. \quad (5.10)$$

4. The associativity law holds: the product between three elements a, b, c can be carried out as the product of one element by the product of the other two or as the product of the product of two elements by the other element, keeping however the order of the elements:

$$a \odot b \odot c = a \odot (b \odot c) = (a \odot b) \odot c. \quad (5.11)$$

The commutativity law in the product of any two elements a, b

$$a \odot b = b \odot a \quad (5.12)$$

can hold or not. If it does, the group is called *Abelian*.

A symmetry is an invariance over a transformation or a group of transformations. In physics, there are well-known symmetries, some related to fundamental properties of space and time. For instance in mechanics, the description of isolated systems is

invariant with respect to space and time translations as well as to space rotations. Noether's theorem grants that for each symmetry of a system there is a corresponding conservation law and therefore a conserved quantity. The formulation of Noether's theorem in quantum mechanics is particularly elegant.

5.3.1 A Quantum Mechanical View of the Noether's Theorem

Suppose that a physical system is invariant under some transformation U (it can be, e.g., the rotation of the coordinate axes). This means that invariance holds when the wave function is subject to the transformation

$$\psi \rightarrow \psi' = U\psi. \quad (5.13)$$

A minimum requirement for U to not change the physical laws is unitarity, since normalization of the wave function should be kept

$$\langle \psi' | \psi' \rangle = \langle U\psi | U\psi \rangle = \langle \psi | U^\dagger U | \psi \rangle = \langle \psi | \psi \rangle \implies U^\dagger U = I \quad (5.14)$$

where I represents the unit operator (which can be, e.g., the identity matrix) and U^\dagger is the Hermitian conjugate of U . We shall use in what follows without distinction the terms Hermitian conjugate, conjugate transpose, Hermitian transpose, or adjoint of an $m \times n$ complex matrix A to indicate the $n \times m$ matrix obtained from A by taking the transpose and then taking the complex conjugate of each entry.

For physical predictions to be unchanged by the symmetry transformation, the eigenvalues of the Hamiltonian should be unchanged; i.e., if

$$\hat{H}\psi_i = E_i\psi_i, \quad (5.15)$$

then

$$\hat{H}\psi'_i = E_i\psi'_i. \quad (5.16)$$

The last equation implies

$$\hat{H}U\psi_i = E_iU\psi_i = UE_i\psi_i = U\hat{H}\psi_i, \quad (5.17)$$

and since, the $\{\psi_i\}$, eigenstates of the Hamiltonian, are a complete basis, U commutes with the Hamiltonian:

$$[\hat{H}, U] = \hat{H}U - U\hat{H} = 0. \quad (5.18)$$

Thus for every symmetry of a system, there is a unitary operator that commutes with the Hamiltonian.

As a consequence, the expectation value of U is constant, since

$$\frac{d}{dt} \langle \psi | U | \psi \rangle = -\frac{i}{\hbar} \langle \psi | [U, H] | \psi \rangle = 0. \quad (5.19)$$

5.3.1.1 Continuum Symmetries

Suppose that U is continuous, and consider the infinitesimal transformation

$$U(\epsilon) = I + i\epsilon G \quad (5.20)$$

(G is called the generator of the transformation U). We shall have, to first order,

$$U^\dagger U \simeq (I - i\epsilon G^\dagger)(I + i\epsilon G) \simeq I + i\epsilon(G - G^\dagger) = I, \quad (5.21)$$

i.e.,

$$G^\dagger = G. \quad (5.22)$$

The generator of the unitary group is thus Hermitian, and it is thus associated to an observable quantity (its eigenvalues are real). Moreover, it commutes with the Hamiltonian:

$$[H, I + i\epsilon G] = 0 \implies [H, G] = 0 \quad (5.23)$$

(trivially $[H, I] = 0$), and since the time evolution of the expectation value of G is given by the equation

$$\frac{d}{dt} \langle G \rangle = \frac{i}{\hbar} \langle [H, G] \rangle = 0 \quad (5.24)$$

the quantity $\langle G \rangle$ is conserved.

Continuum symmetries in quantum mechanics are thus associated to conservation laws related to the group generators. In the next section, we shall make examples; in particular, we shall see how translational invariance entails momentum conservation (the momentum operator being the generator of space translations).

Let us see now how Noether's theorem can be extended to discrete symmetries.

5.3.1.2 Discrete Symmetries

In case one has a discrete Hermitian operator \hat{P} which commutes with the Hamiltonian

$$[\hat{H}, \hat{P}] = 0 \quad (5.25)$$

and a system is in an eigenstate of the operator itself, its time evolution cannot change the eigenvalue.

Let us take for example the parity operator, which will be discussed later. The parity operator, reversing the sign of the space coordinates, is such that

$$\hat{P}^2 = I, \quad (5.26)$$

and thus, its eigenvalues are ± 1 .

Parity-invariant Hamiltonians represent interaction which conserve parity.

Let us examine now some examples of symmetries.

5.3.2 *Some Fundamental Symmetries in Quantum Mechanics*

5.3.2.1 Phase Shift Invariance

In quantum mechanics, a system is described by complex wavefunctions but only the square of their amplitude has physical meaning: it represents the probability density of the system in a point of the space. A global change of the phase of the wave function leaves the system invariant. Indeed, if

$$\psi'(x) = \exp(i\alpha)\psi(x) \quad (5.27)$$

where α is a real number, then

$$\int \psi'^*(x)\psi'(x) dx = \int \psi^*(x) \exp(-i\alpha)\exp(i\alpha)\psi(x) dx = \int \psi^*(x)\psi(x) dx = \langle \psi | \psi \rangle. \quad (5.28)$$

The operator $U = \exp(i\alpha)$ associated to this transformation is a unitary operator: this means that its Hermitian conjugate $U^\dagger = \exp(-i\alpha)$ is equal to its inverse operator U^{-1} .

5.3.2.2 Space Translation Invariance

Due to fundamental properties of space and time, a generic system is invariant with respect to space translations. We can consider, without loss of generality, a translation along x :

$$\psi'(x) = \psi(x + \Delta x) = \psi(x) + \Delta x \frac{\partial}{\partial x} \psi(x) + \frac{1}{2} \Delta x^2 \frac{\partial^2}{\partial x^2} \psi(x) + \dots \quad (5.29)$$

which can be written in a symbolic way as

$$\psi'(x) = \exp\left(\Delta x \frac{\partial}{\partial x}\right)\psi(x). \quad (5.30)$$

The linear momentum operator along x can be expressed as

$$\hat{p}_x = -i\hbar \frac{\partial}{\partial x} \quad (5.31)$$

and thus

$$\psi'(x) = \exp\left(\frac{i}{\hbar}\Delta x \hat{p}_x\right)\psi(x). \quad (5.32)$$

The operator associated to finite space translation Δx along x

$$U_x(\Delta x) = \exp\left(\frac{i}{\hbar}\Delta x \hat{p}_x\right) \quad (5.33)$$

is unitary, and it is said to be generated by the momentum operator \hat{p}_x .

The operator \hat{p}_x commutes with the Hamiltonian of an isolated system, and the associated conserved quantity is the linear momentum p_x .

For an infinitesimal translation δx , just the first terms may be retained and

$$U_x(\delta x) \simeq \left(1 + \frac{i}{\hbar}\delta x \hat{p}_x\right). \quad (5.34)$$

5.3.2.3 Rotational Invariance

The same exercise can be done for other transformations which leave a physical system invariant, like rotations around an arbitrary axis (this invariance is due to isotropy of space). In the case of a rotation about the z -axis, the rotation operator will be

$$R_z(\theta_z) = \exp\left(\frac{i}{\hbar}\theta_z \hat{L}_z\right) \quad (5.35)$$

where \hat{L}_z , the angular momentum operator about the z -axis, is the generator of the rotation:

$$\hat{L}_z = -i\hbar \left(x \frac{\partial}{\partial y} - y \frac{\partial}{\partial x}\right). \quad (5.36)$$

The infinitesimal rotation operator about the z -axis will be then

$$R_z(\delta\theta_z) = \left(1 + \frac{i}{\hbar}\delta\theta_z \hat{L}_z\right). \quad (5.37)$$

It can be shown that in rectangular coordinates (x, y, z) , the angular momentum can be replaced in the perturbative expansion of the rotation by the matrix

$$\hat{L}_z = \hbar \begin{pmatrix} 0 & -i & 0 \\ i & 0 & 0 \\ 0 & 0 & 0 \end{pmatrix} \quad (5.38)$$

so that, expanding the exponential, the usual rotation matrix is recovered:

$$R_z(\theta_z) = \exp\left(\frac{i}{\hbar}\theta_z\hat{L}_z\right) = \begin{pmatrix} \cos\theta_z & \sin\theta_z & 0 \\ -\sin\theta_z & \cos\theta_z & 0 \\ 0 & 0 & 1 \end{pmatrix}. \quad (5.39)$$

A sequence of rotations about axes x , y , and z is described by the product of the corresponding operators:

$$R_x(\theta_x) R_y(\theta_y) R_z(\theta_z) = \exp\left(\frac{i}{\hbar}\theta_x\hat{L}_x\right) \exp\left(\frac{i}{\hbar}\theta_y\hat{L}_y\right) \exp\left(\frac{i}{\hbar}\theta_z\hat{L}_z\right) \quad (5.40)$$

which is, as the angular operators do not commute, different from the exponential of the sum of the exponents

$$R_x(\theta_x) R_y(\theta_y) R_z(\theta_z) \neq \exp\left[\frac{i}{\hbar}\left(\theta_x\hat{L}_x + \theta_y\hat{L}_y + \theta_z\hat{L}_z\right)\right]; \quad (5.41)$$

The result of a sequence of rotations depends on the order in which the rotations are done. Being \hat{A} and \hat{B} two operators, the following relation holds:

$$\exp(\hat{A} + \hat{B}) = \exp\left(\frac{1}{2}[\hat{A}, \hat{B}]\right) \exp(\hat{A}) \exp(\hat{B}) \quad (5.42)$$

where $[\hat{A}, \hat{B}]$ is the commutator of the two operators.

The commutators of the angular momentum operators are indeed not zero and given by

$$[\hat{L}_x, \hat{L}_y] = i\hbar\hat{L}_z; \quad [\hat{L}_y, \hat{L}_z] = i\hbar\hat{L}_x; \quad [\hat{L}_z, \hat{L}_x] = i\hbar\hat{L}_y. \quad (5.43)$$

The commutation relations between the generators determine thus the product of the elements of the rotation group and are known as the Lie algebra of the group.

Once a basis is defined, operators can in most cases be associated to matrices; there is a isomorphism between vectors and states, matrices and operators.² In the

²Here, we are indeed cutting a long story short; we address the interested readers to a textbook in quantum physics to learn what is behind this fundamental point.

following, whenever there is no ambiguity, we shall identify operators and matrices, and we shall omit when there is no ambiguity the “hat” associated to operators.

5.3.3 Unitary Groups and Special Unitary Groups

Unitary groups $U(n)$ and Special Unitary groups $SU(n)$ of a generic rank n play a central role in particle physics both related to the classification of the elementary particles and to the theories of fundamental interactions.

The unitary group $U(n)$ is the group of unitary complex square matrices with n rows and n columns. A complex $n \times n$ matrix has $2n^2$ parameters, but the unitarity condition ($U^\dagger U = U U^\dagger = 1$) imposes n^2 constraints, and thus, the number of free parameters is n^2 . A particularly important group is the group $U(1)$ which has just one free parameter and so one generator. It corresponds to a phase transformation:

$$U = \exp\left(\frac{i}{\hbar}\alpha\hat{A}\right) \quad (5.44)$$

where α is a real number and \hat{A} is a Hermitian operator. Relevant cases are \hat{A} being the identity operator (like a global change of the phase of the wave function as discussed above) or an operator associated to a single measurable quantity (like the electric charge or the baryonic number). Noether’s theorem ensures that the invariance of the Hamiltonian with respect to such transformation entails the conservation of a corresponding measurable quantity.

The special unitary group $SU(n)$ is the group of unitary complex matrices of dimension $n \times n$ and with determinant equal to 1. The number of free parameters and generators of the group is thus $(n^2 - 1)$. Particularly important groups will be the groups $SU(2)$ and $SU(3)$.

5.3.4 $SU(2)$

$SU(2)$ is the group of the spin rotations. The generic $SU(2)$ matrix can be written as

$$\begin{pmatrix} a & b \\ -b^* & a^* \end{pmatrix} \quad (5.45)$$

where a and b are complex numbers and $|a|^2 + |b|^2 = 1$. This group has three free parameters and thus three generators. $SU(2)$ operates in an internal space of particle *spinors*, which in this context are complex two-dimensional vectors introduced to describe the spin $\frac{1}{2}$ (as the electron) polarization states. For instance in a $(|z\rangle, |-z\rangle)$ basis, the polarization states along z , x , and y can be written as

$$\begin{aligned}
|+z\rangle &= \begin{pmatrix} 1 \\ 0 \end{pmatrix}; & |-z\rangle &= \begin{pmatrix} 0 \\ 1 \end{pmatrix} \\
|+x\rangle &= \frac{1}{\sqrt{2}} \begin{pmatrix} 1 \\ 1 \end{pmatrix}; & |-x\rangle &= \frac{1}{\sqrt{2}} \begin{pmatrix} 1 \\ -1 \end{pmatrix} \\
|+y\rangle &= \frac{1}{\sqrt{2}} \begin{pmatrix} 1 \\ i \end{pmatrix}; & |-y\rangle &= \frac{1}{\sqrt{2}} \begin{pmatrix} 1 \\ -i \end{pmatrix}.
\end{aligned}$$

The generators of the group, which are the spin $\frac{1}{2}$ angular momentum operators, can be for example (it is not a unique choice) the Pauli matrices σ_z , σ_x e and σ_y

$$\sigma_z = \begin{pmatrix} 1 & 0 \\ 0 & -1 \end{pmatrix}; \quad \sigma_x = \begin{pmatrix} 0 & 1 \\ 1 & 0 \end{pmatrix}; \quad \sigma_y = \begin{pmatrix} 0 & -i \\ i & 0 \end{pmatrix}, \quad (5.46)$$

being

$$\hat{S}_z = \frac{\hbar}{2}\sigma_z; \quad \hat{S}_x = \frac{\hbar}{2}\sigma_x; \quad \hat{S}_y = \frac{\hbar}{2}\sigma_y. \quad (5.47)$$

The following commutation relations hold:

$$[\hat{S}_i, \hat{S}_j] = i\hbar \varepsilon_{ijk} \hat{S}_k \quad (5.48)$$

where ε_{ijk} , the Levi-Civita symbol, is the completely antisymmetric matrix which takes the value 1 if i, j, k , is obtained by an even number of permutations of x, y, z , the value -1 if i, j, k , is obtained by a odd number for permutations of x, y, z , and is zero otherwise.

These commutation relations are identical to those discussed above for the generators of space rotations (the normal angular momentum operators) in three dimensions, which form a SO(3) group (group of real orthogonal matrices of dimension 3×3 with determinant equal to 1). SU(2) and SO(3) have thus the same algebra, and there is a mapping between the elements of SU(2) and elements of SO(3) which respect the respective group operations. But, while in our example SO(3) operates in the real space transforming particle wave functions, SU(2) operates in the internal space of particle spinors.

The rotation operator in this spinor space around a generic axis j can then be written as

$$U = \exp\left(i\frac{\theta_j}{2}\sigma_j\right), \quad (5.49)$$

and in general, defining $\boldsymbol{\sigma} = \sigma_x \mathbf{e}_x + \sigma_y \mathbf{e}_y + \sigma_z \mathbf{e}_z$ where the $\mathbf{e}_{x,y,z}$ are the unit vectors of the coordinate axes, and aligning the rotation axis to a unit vector \mathbf{n} :

$$U = \exp\left(i\frac{\theta}{2}\mathbf{n} \cdot \boldsymbol{\sigma}\right) = \cos\frac{\theta}{2} + i\sin\frac{\theta}{2}\mathbf{n} \cdot \boldsymbol{\sigma} \quad (5.50)$$

where the cosine term is implicitly multiplied by the identity 2×2 matrix.

Spin projection operators do not commute, and thus, the Heisenberg theorem tells us that the projection of the spin along different axis cannot be measured simultaneously with arbitrary precision. However, there are $(n - 1)$ operators (called the Casimir operators) which do commute with all the SU(n) generators. Then in the case of SU(2) there is one Casimir operator which is usually chosen as the square of the total spin:

$$\hat{S}^2 = \hat{S}_x^2 + \hat{S}_y^2 + \hat{S}_z^2. \quad (5.51)$$

This operator has eigenvalues $s(s + 1)$ where s is the total spin:

$$\hat{S}^2 |s, m_s\rangle = \hbar^2 s(s + 1) |s, m_s\rangle. \quad (5.52)$$

If \hat{S}_z is chosen as the projection operator

$$\hat{S}_z |s, m_s\rangle = \hbar m_s |s, m_s\rangle. \quad (5.53)$$

Spin eigenstates can be thus labeled by the eigenvalues m_s of the projection operator along a given axis and by the total spin s . The two other operators \hat{S}_x and \hat{S}_y can be combined forming the so-called raising and lowering operators \hat{S}_+ and \hat{S}_- :

$$\hat{S}_+ = \hat{S}_x + i\hat{S}_y \quad (5.54)$$

$$\hat{S}_- = \hat{S}_x - i\hat{S}_y. \quad (5.55)$$

The names “raising” and “lowering” are justified by the fact that

$$\hat{S}_z \hat{S}_+ |s, m_s\rangle = \hbar (m_s + 1) \hat{S}_+ |s, m_s\rangle \quad (5.56)$$

$$\hat{S}_z \hat{S}_- |s, m_s\rangle = \hbar (m_s - 1) \hat{S}_- |s, m_s\rangle \quad (5.57)$$

and

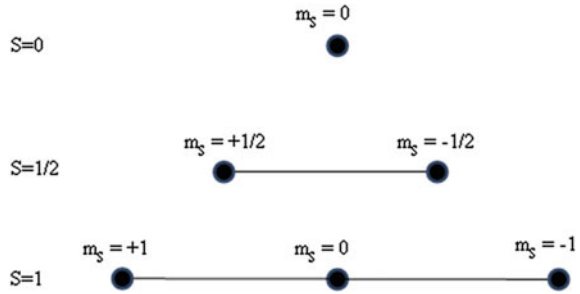
$$\hat{S}_+ |s, m_s\rangle = \hbar \sqrt{(s - m_s)(s + m_s + 1)} |s, m_s + 1\rangle \quad (5.58)$$

$$\hat{S}_- |s, m_s\rangle = \hbar \sqrt{(s + m_s)(s - m_s + 1)} |s, m_s - 1\rangle. \quad (5.59)$$

Particles with spins higher than $\frac{1}{2}$ have to be accommodated in SU(n) representations of higher order. For example, for spin 1 particles, the spin projection operator has three eigenvalues (1, 0, -1) and therefore the spin states are described by a three-component vector. In this case, the spin operators are 3×3 matrices. For instance, in a $|z\rangle$ basis:

$$\hat{S}_z = \begin{pmatrix} 1 & 0 & 0 \\ 0 & 0 & 0 \\ 0 & 0 & -1 \end{pmatrix}; \quad \hat{S}_x = \frac{1}{\sqrt{2}} \begin{pmatrix} 0 & -1 & 0 \\ -1 & 0 & 1 \\ 0 & 1 & 0 \end{pmatrix}; \quad \hat{S}_y = \frac{i}{\sqrt{2}} \begin{pmatrix} 0 & 1 & 0 \\ -1 & 0 & -1 \\ 0 & 1 & 0 \end{pmatrix} \quad (5.60)$$

Fig. 5.2 Graphical representation of SU(2) multiplets



which have the same commutation relation as the 2×2 fundamental representation.

A graphical representation of a spin s multiplet can be done as $(2s + 1)$ nodes aligned along an axis m_s (Fig. 5.2).

5.3.5 SU(3)

SU(3) is the group behind the so-called eightfold way (the organization of baryons and mesons in octets and decuplets, which was the first successful attempt of classification of hadrons) and behind QCD (quantum chromodynamics, the modern theory of strong interactions). Indeed, SU(3) operates in an internal space of three-dimensional complex vectors and thus can accommodate at the same level rotations among three different elements (flavors u, d, s or colors Red, Green, Blue). The eightfold way will be discussed later in this chapter, while QCD will be discussed in Chap. 6; here, we present the basics of SU(3).

The elements of SU(3) generalizing SU(2) can be written as

$$U_j = \exp\left(i\frac{\theta_j}{2}\lambda_j\right), \tag{5.61}$$

where the 3×3 matrices λ_j are the generators. Since for a generic matrix A

$$\det(e^A) = e^{\text{tr}(A)}, \tag{5.62}$$

the λ_j matrices should be traceless. SU(3) has thus $3^2 - 1 = 8$ traceless, and Hermitian generators that in analogy with SU(2) Pauli matrices can be defined as

$$t_i = \frac{\hbar}{2}\lambda_i, \tag{5.63}$$

where λ_i are the Gell-Mann matrices:

$$\lambda_1 = \begin{pmatrix} 0 & 1 & 0 \\ 1 & 0 & 0 \\ 0 & 0 & 0 \end{pmatrix}; \lambda_2 = \begin{pmatrix} 0 & -i & 0 \\ i & 0 & 0 \\ 0 & 0 & 0 \end{pmatrix}; \lambda_3 = \begin{pmatrix} 1 & 0 & 0 \\ 0 & -1 & 0 \\ 0 & 0 & 0 \end{pmatrix} \tag{5.64}$$

$$\lambda_4 = \begin{pmatrix} 0 & 0 & 1 \\ 0 & 0 & 0 \\ 1 & 0 & 0 \end{pmatrix}; \lambda_5 = \begin{pmatrix} 0 & 0 & -i \\ 0 & 0 & 0 \\ i & 0 & 0 \end{pmatrix} \tag{5.65}$$

$$\lambda_6 = \begin{pmatrix} 0 & 0 & 0 \\ 0 & 0 & 1 \\ 0 & 1 & 0 \end{pmatrix}; \lambda_7 = \begin{pmatrix} 0 & 0 & 0 \\ 0 & 0 & -i \\ 0 & i & 0 \end{pmatrix}; \lambda_8 = \frac{1}{\sqrt{3}} \begin{pmatrix} 1 & 0 & 0 \\ 0 & 1 & 0 \\ 0 & 0 & -2 \end{pmatrix} \tag{5.66}$$

and have the following commutation relations:

$$(\lambda_i, \lambda_j) = 2i \sum_k f_{ijk} \lambda_k \tag{5.67}$$

where the nonzero *structure constants* f_{ijk} are permutations of the following:

ijk	123	147	156	246	257	345	367	458	678
f_{ijk}	1	$1/2$	$-1/2$	$1/2$	$1/2$	$1/2$	$-1/2$	$\sqrt{3}/2$	$\sqrt{3}/2$

(5.68)

SU(3) contains three SU(2) subgroups corresponding to the different rotations between any pair of the three group elements. Note for instance that the first three λ matrices are built as the extension of the SU(2) generators we have discussed before.

The generators λ_3 and λ_8 commute, and thus, they have common eigenstates; their eigenvalues can thus be used to label the eigenstates. We call the corresponding quantum numbers “third isospin component” I_3 and “hypercharge” Y quantum numbers. The other operators can be, in a similar way as it was done for SU(2), combined two by two to form raising and lowering (step) operators. Then the *standard* SU(3) generators will be defined as:

$$\hat{I}_3 = t_3; \hat{Y} = \frac{2}{\sqrt{3}}t_8 \tag{5.69}$$

$$\hat{I}_\pm = t_1 \pm it_2 \tag{5.70}$$

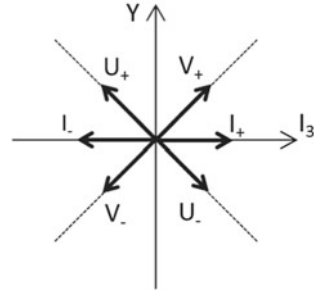
$$\hat{V}_\pm = t_4 \pm it_5 \tag{5.71}$$

$$\hat{U}_\pm = t_6 \pm it_7. \tag{5.72}$$

The step operators act as follows:

- \hat{I}_\pm leaves Y unchanged and changes \hat{I}_3 by ± 1 ,
- \hat{V}_\pm changes Y by ± 1 and changes \hat{I}_3 by $\pm 1/2$,
- \hat{U}_\pm changes Y by ± 1 and changes \hat{I}_3 by $\pm 1/2$.

Fig. 5.3 Graphical representation of the SU(3) step operators



Graphically, these operations can be represented as vectors in a (I_3, Y) space (Fig. 5.3). SU(3) multiplets form then in this space plane figures (triangles, octagons, ...) as it will be discussed later on (Figs. 5.7 and 5.8).

5.3.6 Discrete Symmetries: Parity, Charge Conjugation, and Time Reversal

Let us examine now in larger detail three fundamental discrete symmetries: parity, charge conjugation, and time reversal.

5.3.6.1 Parity

We have already introduced the parity transformation (sometimes called wrongly “mirror reflection”), which reverses all spatial coordinates:

$$\mathbf{x} \rightarrow \mathbf{x}' = -\mathbf{x}. \tag{5.73}$$

A *vector* (for instance, the position vector, the linear momentum or the electric field) will be inverted under parity transformation, while the cross product of two vectors (like the angular momentum or the magnetic field) will not be changed. The latter is called *pseudo—(or axial) vector*. The internal product of two vectors is a *scalar* and is invariant under parity transformation but the internal product of a vector and a pseudo-vector changes sign under parity transformation and thus it is called a *pseudo-scalar*.

The application of the parity operator \hat{P} once and twice to a wave function leads to

$$\begin{aligned} \hat{P}\psi(\mathbf{x}) &= \psi(-\mathbf{x}) = \lambda_P \psi(\mathbf{x}) \\ \hat{P}^2\psi(\mathbf{x}) &= \lambda_P^2 \psi(\mathbf{x}) = \psi(\mathbf{x}) \end{aligned}$$

implying that the eigenvalues of the \hat{P} operator are $\lambda_P = \pm 1$. The parity group has just two elements: \hat{P} and the identity operator \hat{I} . \hat{P} is thus Hermitian, and a measurable quantity, *parity*, can be associated to its eigenvalues: parity is a legal quantum number.

Electromagnetic and strong interactions appear to be invariant under parity transformations (and therefore the parity quantum number is conserved in these interactions) but, as it will be discussed in the next chapter, weak interactions, with the surprise of most of physicists in the 1950s, are not.

For any system bound by a central potential, $V(r)$, the spatial part of the wave function can be written as the product of a radial and an angular part, with the angular part described by spherical harmonics:

$$\psi(r, \theta, \phi) = R(r)Y_m^l(\theta, \phi). \quad (5.74)$$

The parity operator in polar coordinates changes from θ to $\pi - \theta$ and ϕ to $\pi + \phi$. One can prove that

$$\hat{P}Y_m^l = (-1)^l Y_m^l. \quad (5.75)$$

Elementary particles are (with good approximation) eigenstates of \hat{P} , since a generic free-particle Hamiltonian is with good approximation parity invariant, and an “intrinsic” parity is assigned to each particle. Fermions and antifermions have opposite parities; bosons and antibosons have the same parity.

The photon has a negative parity: this can be seen by the fact that the basic atomic transition is characterized by the emission of a photon and a change of orbital angular momentum by one unit. All vector bosons have a negative parity, while the axial vector bosons have a positive parity.

Example: Experimental Determination of the Pion Parity. By convention, we define that protons and neutrons have positive intrinsic parity. The negative parity of pions can be determined by assuming parity and angular momentum conservation in the capture at rest of a π^- by a deuterium nucleus producing two neutrons in the final state ($\pi^- d \rightarrow nn$). The parity of a system of two particles is the product of the parities of the two particles multiplied by a $(-1)^l$ factor where l is the orbital angular momentum of the system ($l = 0$ is the ground state). In the case of the nn system discussed above, $l = 1$ and thus the final state parity is -1 . Pseudo-scalar mesons (like pions) have negative parity, while scalar mesons have positive parity.

Combining Parity in a set of Particles. Parity is a multiplicative quantum number contrary to, for instance, electric charge which is additive. In fact, while discrete symmetry groups are usually defined directly by the corresponding operators, continuous symmetry groups are, as it was seen, associated to the exponentiation of generators,

$$U = \exp\left(\frac{i}{\hbar}\alpha\hat{Q}\right). \quad (5.76)$$

5.3.6.2 Charge Conjugation

Charge conjugation reverses the sign of all “internal” quantum numbers (electric charge, baryon number, strangeness, ...) keeping the values of mass, momentum, energy, and spin. It transforms a particle in its own antiparticle. Applying the charge conjugation operator \hat{C} twice brings the state back to its original state, as in the case of parity. The eigenvalues of \hat{C} are again $\lambda_C = \pm 1$, but most of the elementary particles are not eigenstates of \hat{C} (particle and antiparticle are not usually the same); this is trivial for electrically charged particles.

Once again electromagnetic and strong interactions appear to be invariant under charge conjugation, but weak interactions are not (they are “almost” invariant with respect to the product $\hat{C}\hat{P}$ as it will be discussed later on).

Electric charge changes sign under charge conjugation and so do electric and magnetic fields. The photon has thus a negative \hat{C} eigenvalue. The neutral pion π^0 decays into two photons: its \hat{C} eigenvalue is positive. Now you should be able to answer the question: is the decay $\pi^0 \rightarrow \gamma\gamma$ possible?

5.3.6.3 Time Reversal and *CPT*

Time reversal inverts the time coordinate:

$$t \rightarrow t' = -t. \quad (5.77)$$

Physical laws that are invariant under such transformation have no preferred time direction. Going back in the past would be as possible as going further in the future. Although we have compulsory evidence in our lives that this is not the case, the Hamiltonians of fundamental interactions were believed to exhibit such invariance. On the other hand, in relativistic quantum field theory in flat space–time geometry, it has been demonstrated (*CPT* theorem), under very generic assumptions, that any quantum theory is invariant under the combined action of charge conjugation, space reversal, and time reversal. This is the case of the Standard Model of particle physics. As a consequence of the *CPT* theorem, particles and antiparticles must have identical masses and lifetimes. Stringent tests have been performed being the best the limit at 90 % CL on the mass difference between the K^0 and the \bar{K}^0 :

$$\left| \frac{m_{K^0} - m_{\bar{K}^0}}{1/2(m_{K^0} + m_{\bar{K}^0})} \right| < 0.6 \times 10^{-18}. \quad (5.78)$$

So far *CPT* remains both experimentally and theoretically an exact symmetry. This implies that any violation of one of the individual symmetries (*C*, *P*, *T*) must be compensated by corresponding violation(s) in at least one of the others symmetries. In the late 1950s, and early 1960s, it was found that *P* and *C* are individually violated in weak interactions and that, beyond all the expectations, their combined action (*CP*) is also violated in particular particle systems (see Sect. 6.3.8). Therefore, *T* should

be also violated in such systems. Indeed, the T violation has been recently detected in the B meson sector. The arrow of time is also manifest at the level of fundamental particles.

5.3.7 Isospin

In 1932, J. Chadwick discovered the neutron after more than 10 years of intensive experimental searches following the observation by Rutherford that to explain the mass and charges of all atoms, and excluding hydrogen, the nucleus should consist of protons and of neutral bound states of electrons and protons. The particle discovered was not a bound state of electron and proton—meanwhile, the uncertainty relations demonstrated by Heisenberg in 1927 had indeed forbidden it. The neutron was indeed a particle like the proton with almost the same mass ($m_p \simeq 939.57 \text{ MeV}/c^2$, $m_n \simeq 938.28 \text{ MeV}/c^2$), the same behavior with respect to nuclear interaction, but with no electric charge. It was the neutral “brother” of the proton.

Soon after neutron discovery, Heisenberg proposed to regard proton and neutron as two states of a single particle later on called the *nucleon*. The formalism was borrowed from the Pauli spin theory and Wigner, in 1937, called “isospin” symmetry this new internal symmetry with respect to rotations in the space defined by the vectors $(p, 0)$ and $(0, n)$. Strong interactions should be invariant with respect to an internal $SU(2)$ symmetry group, the nucleons would have isospin $I = 1/2$, and their states would be described by isospin spinors. By convention, the proton is identified with the isospin-up ($I_3 = +1/2$) projection and the neutron with the isospin-down ($I_3 = -1/2$) projection.

As we have discussed in Chap. 3, Yukawa postulated in 1935 that the short-range nuclear interaction might be explained by the exchange of a massive meson, the pion. The charge independence of nuclear interactions suggested later on that three pions (π^+ , π^- , π^0) should exist. Nuclear interaction could thus be seen as an interaction between the nucleon isospin doublet ($I = 1/2$) and a isovector ($I = 1$) triplet of pions. Three spin 0 and isospin 1 pions (π^+ with $I_3 = +1$, π^0 with $I_3 = 0$, π^- with $I_3 = -1$) with almost the same masses ($m_{\pi^\pm} \simeq 139.6 \text{ MeV}/c^2$, $m_{\pi^0} \simeq 135.0 \text{ MeV}/c^2$) were indeed discovered in the late 1940s and in the beginning of the 1950s. The isospin theory of nuclear interactions was established.

5.3.7.1 The Isospin of a System of Particles

The isospin of a system of particles can be expressed as a function of the isospin of the individual particles using the same addition rules valid for the sum of ordinary spins or angular momenta.

In a system of two particles, the projection of the total spin of the system on an axis (conventionally assumed to be the z axis) is just the sum of the projections of the individual spins, $m_s = m_{s_1} + m_{s_2}$, while the total spin s can take values from

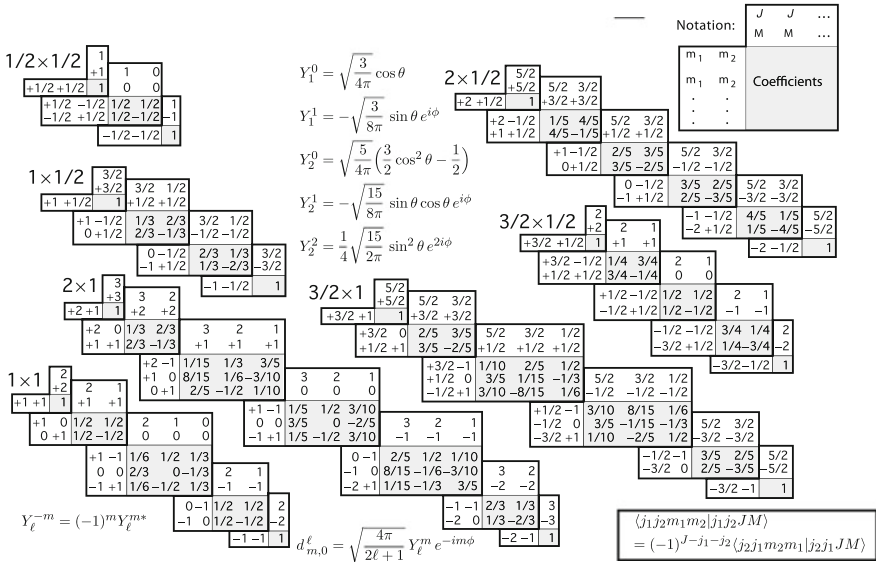


Fig. 5.4 Clebsch–Gordan coefficients and spherical harmonics. From K.A. Olive et al. (Particle Data Group), Chin. Phys. C 38 (2014) 090001. Note: a square-root sign is to be understood over every coefficient, e.g., for $-8/15$ read $-\sqrt{8/15}$

$|s_1 - s_2|$ to $s_1 + s_2$. The weights of the different final states in the total amplitude are given by the squares of the so-called Clebsch–Gordan coefficients C_{sm,s_1m_1,s_2m_2} . The calculation of these coefficients is not relevant for the purpose of this book; they can be found in tables, an example being given in Fig. 5.4.

For example, the addition of two spin $\frac{1}{2}$ particles gives

$$\left| \frac{1}{2}, \frac{1}{2} \right\rangle + \left| \frac{1}{2}, \frac{1}{2} \right\rangle = |1, 1\rangle$$

$$\left| \frac{1}{2}, \frac{1}{2} \right\rangle + \left| \frac{1}{2}, -\frac{1}{2} \right\rangle = \frac{1}{\sqrt{2}} |1, 0\rangle + \frac{1}{\sqrt{2}} |0, 0\rangle$$

$$\left| \frac{1}{2}, -\frac{1}{2} \right\rangle + \left| \frac{1}{2}, \frac{1}{2} \right\rangle = \frac{1}{\sqrt{2}} |1, 0\rangle - \frac{1}{\sqrt{2}} |0, 0\rangle$$

$$\left| \frac{1}{2}, -\frac{1}{2} \right\rangle + \left| \frac{1}{2}, -\frac{1}{2} \right\rangle = |1, -1\rangle$$

The final states can be organized in a symmetric triplet of total spin 1

$$|1, 1\rangle = \left| \frac{1}{2}, \frac{1}{2} \right\rangle \left| \frac{1}{2}, \frac{1}{2} \right\rangle$$

$$|1, 0\rangle = \frac{1}{\sqrt{2}} \left| \frac{1}{2}, \frac{1}{2} \right\rangle \left| \frac{1}{2}, -\frac{1}{2} \right\rangle + \frac{1}{\sqrt{2}} \left| \frac{1}{2}, -\frac{1}{2} \right\rangle \left| \frac{1}{2}, \frac{1}{2} \right\rangle \quad (5.79)$$

$$|1, -1\rangle = \left| \frac{1}{2}, -\frac{1}{2} \right\rangle \left| \frac{1}{2}, -\frac{1}{2} \right\rangle$$

and in an antisymmetric singlet of total spin 0

$$|0, 0\rangle = \frac{1}{\sqrt{2}} \left| \frac{1}{2}, \frac{1}{2} \right\rangle \left| \frac{1}{2}, -\frac{1}{2} \right\rangle - \frac{1}{\sqrt{2}} \left| \frac{1}{2}, -\frac{1}{2} \right\rangle \left| \frac{1}{2}, \frac{1}{2} \right\rangle. \quad (5.80)$$

In the language of group theory, the direct product of two SU(2) doublets gives a triplet and a singlet:

$$2 \otimes 2 = 3 \oplus 1. \quad (5.81)$$

5.3.7.2 Isospin and Cross Section

Strong interactions are invariant under SU(2) rotations in the internal isospin space and according to Noether's theorem, total isospin is conserved in such interactions. The transition amplitudes between initial and final states are a function of the isospin I and can be labeled as \mathcal{M}_I .

Let us consider the inelastic collision of two nucleons giving a deuterium nucleus and a pion. Three channels are considered:

1. $p + p \rightarrow d + \pi^+$
2. $p + n \rightarrow d + \pi^0$
3. $n + n \rightarrow d + \pi^-$.

The deuteron d is a pn bound state and must have isospin $I = 0$; otherwise, the bound states pp and nn should exist (experimentally, they do not exist). The isospin quantum numbers $|I, I_3\rangle$ of the final states are thus those of the π , which means $|1, 1\rangle$, $|1, 0\rangle$, $|1, -1\rangle$, respectively. The isospins of the initial states follow the rules of the addition of two isospin 1/2 states discussed above, and are, respectively, $|1, 1\rangle$, $\frac{1}{\sqrt{2}}|1, 0\rangle + \frac{1}{\sqrt{2}}|0, 0\rangle$ and $|1, -1\rangle$. As the final state is a pure $I = 1$ state, only the transition amplitude corresponding to $I = 1$ is possible. The cross section (proportional to the square of the sum of the scattering amplitudes) for the reaction $p + n \rightarrow d + \pi^0$ should then be half of each of the cross sections of any of the other reactions.

Let us consider now the $\pi^+ p$ and $\pi^- p$ collisions:

1. $\pi^+ + p \rightarrow \pi^+ + p$
2. $\pi^- + p \rightarrow \pi^- + p$
3. $\pi^- + p \rightarrow \pi^0 + n$.

Using the Clebsch–Gordan tables, the isospin decomposition of the initial and final states are

$$\begin{aligned} \pi^+ + p &: |1, 1\rangle + \left| \frac{1}{2}, \frac{1}{2} \right\rangle = \left| \frac{3}{2}, \frac{3}{2} \right\rangle \\ \pi^- + p &: |1, -1\rangle + \left| \frac{1}{2}, \frac{1}{2} \right\rangle = \sqrt{\frac{1}{3}} \left| \frac{3}{2}, -\frac{1}{2} \right\rangle - \sqrt{\frac{2}{3}} \left| \frac{1}{2}, -\frac{1}{2} \right\rangle \\ \pi^0 + n &: |1, 0\rangle + \left| \frac{1}{2}, -\frac{1}{2} \right\rangle = \sqrt{\frac{2}{3}} \left| \frac{3}{2}, -\frac{1}{2} \right\rangle + \sqrt{\frac{1}{3}} \left| \frac{1}{2}, -\frac{1}{2} \right\rangle. \end{aligned}$$

Therefore, there are two possible transition amplitudes $\mathcal{M}_{1/2}$ and $\mathcal{M}_{3/2}$ corresponding to $I = \frac{1}{2}$ and $I = \frac{3}{2}$, respectively, and

$$\begin{aligned} \mathcal{M}(\pi^+ p \rightarrow \pi^+ p) &\propto \mathcal{M}_{3/2} \\ \mathcal{M}(\pi^- p \rightarrow \pi^- p) &\propto \frac{1}{3} \mathcal{M}_{3/2} + \frac{2}{3} \mathcal{M}_{1/2} \\ \mathcal{M}(\pi^- p \rightarrow \pi^0 n) &\propto \frac{\sqrt{2}}{3} \mathcal{M}_{3/2} - \frac{\sqrt{2}}{3} \mathcal{M}_{1/2}. \end{aligned}$$

Experimentally, in 1951, the group led by Fermi in Chicago discovered in the $\pi^+ p$ elastic scattering channel an unexpected and dramatic increase at center-of-mass energies of 1232 MeV (Fig. 5.5). Such increase was soon after interpreted by Keith Brueckner (Fermi was not convinced) as evidence that the pion and the proton form at that energy a short-lived bound state with isospin number $I = \frac{3}{2}$. Indeed, whenever $\mathcal{M}_{3/2} \gg \mathcal{M}_{1/2}$,

Fig. 5.5 Total cross section for the collision of positive and negative pions with protons as a function of the pion kinetic energy. Credit: E.M Henley and A. Garcia, Subatomic physics, World Scientific 2007

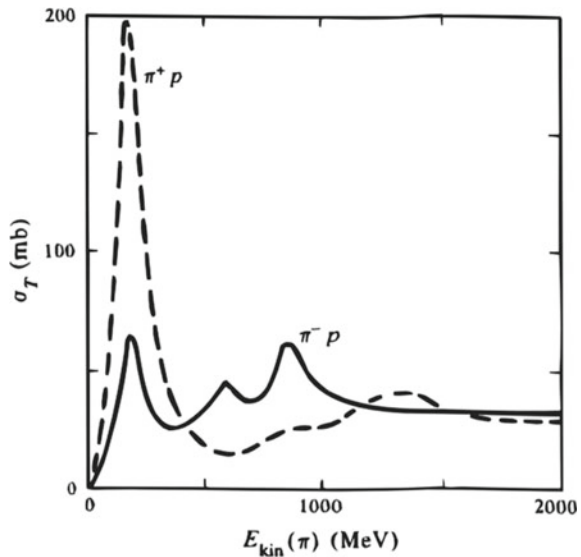
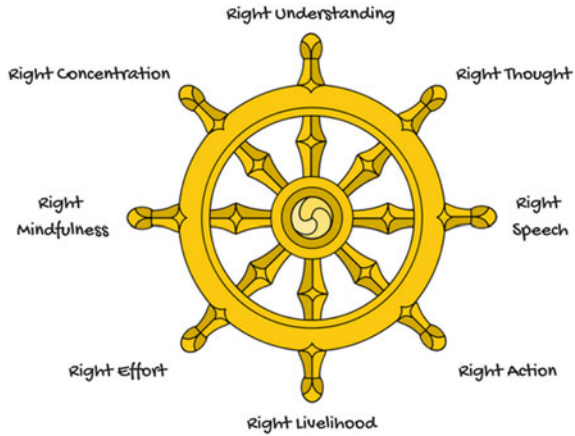


Fig. 5.6 Dharma wheel representing the Buddhist “eightfold path” to liberation from pain. From Wikimedia Commons



$$\frac{\sigma(\pi^+ p \rightarrow \pi^+ p)}{\sigma(\pi^- p \rightarrow \pi^- p) + \sigma(\pi^- p \rightarrow \pi^0 p)} \sim \frac{\mathcal{M}_{3/2}^2}{\frac{1}{9}\mathcal{M}_{3/2}^2 + \frac{2}{9}\mathcal{M}_{3/2}^2} \sim 3$$

in agreement with the measured value of such ratio as shown in Fig. 5.5.

This resonance is now called the Δ ; being a $I = \frac{3}{2}$ state it has, as expected, four projections, called $\Delta^{++}, \Delta^+, \Delta^0, \Delta^-$.

5.3.8 The Eightfold Way

The “eightfold way” is the name Murray Gell-Mann, inspired by the noble eightfold path from the Buddhism (Fig. 5.6), gave to the classification of mesons and baryons proposed independently by him, by Yuval Ne’eman and by André Petermann in the early 1960s.

As discussed in Chap. 3, strange particles had been discovered in the late 1940s in cosmic rays, and later abundantly produced in early accelerator experiments in the beginning of the 1950s. These particles were indeed strange considering the knowledge at that time: they have large masses, and they are produced in pairs with large cross sections, but they have large lifetimes as compared with what expected for nuclear resonances. Their production is ruled by strong interactions while they decay weakly. A new quantum number, *strangeness*, was assigned in 1953 to these particles by Nakano and Nishijima and, independently, by Gell-Mann. By convention, positive K mesons (kaons) have strangeness +1, while Λ baryons have strangeness -1. “Ordinary” (nonstrange) particles (proton, neutron, pions, . . .) have strangeness 0.

Strangeness is conserved in the associated production of kaons and lambdas, as for instance, in

$$\pi^+ n \rightarrow K^+ \Lambda ; \pi^- p \rightarrow K^0 \Lambda \tag{5.82}$$

but not conserved in strange particle decays, e.g.,

$$\Lambda \rightarrow \pi^- p ; K^0 \rightarrow \pi^- \pi^+ . \tag{5.83}$$

Strange particles can also be grouped in isospin multiplets, but the analogy with strangeless particles is not straightforward. Pions are grouped in an isospin triplet being the π^+ the antiparticle of the π^- and the π^0 its own antiparticle. For kaons, the existence of the strangeness quantum number implies that there are four different states which are organized in two isospin doublets: (K^+, K^0) and (K^-, \bar{K}^0) having, respectively, strangeness $S = +1$ and $S = -1$ and being the antiparticles of each other.

Gell-Mann and Nishijima noticed also that there is an empirical relation between the electric charge, the third component of isospin I_3 , and a new quantum number, the hypercharge $Y = B + S$, defined as the sum of the baryonic number B (being $B = 0$ for mesons, $B = 1$ for baryons and $B = -1$ for antibaryons) and strangeness S :

$$Q = I_3 + \frac{1}{2}Y .$$

The known mesons and baryons with the same spin and parity were then grouped forming geometrical hexagons and triangles in the (I_3, Y) plane (examples in Figs. 5.7 and 5.8). The masses of the particles in each multiplet were similar but not strictly equal (they would be if the symmetry were perfect). Indeed, while particles lying on the horizontal lines with the same isospin have almost equal masses, the masses of the particles in consecutive horizontal lines differ by 130–150 MeV/c².

In the middle of each hexagon, there are two particles with $I_3 = 0, Y = 0$: one with $I = 0$ (η^0, Λ) and one with $I = 1$ (π^0, Σ^0). In the triangle (decuplet) 10 spin 3/2 baryons could be accommodated.

There was however an empty spot in the decuplet: a baryon with $Q = -1, I = 0, Y = -2, S = -3$ and a mass around 1670 MeV/c² was missing. This particle, which we call now the Ω^- , was indeed discovered in the Brookhaven National Laboratory 2-meter hydrogen bubble chamber in 1964 (Fig. 5.9). A K^- meson interacts with a

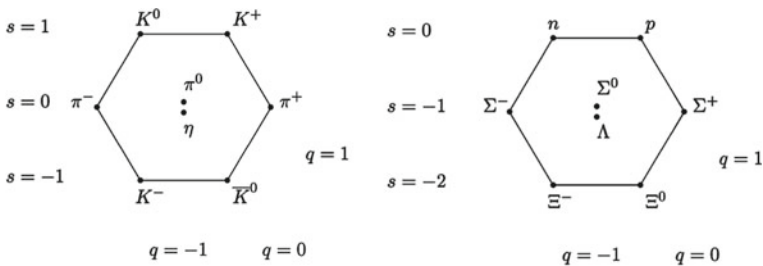


Fig. 5.7 Fundamental meson and baryon octets: on the left spin 0, parity -1 (pseudo-scalar mesons); on the right the spin 1/2 baryons. The I_3 axis is the abscissa, while the Y axis is the ordinate

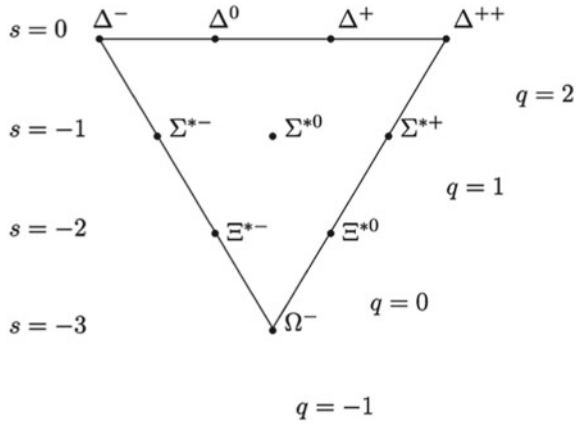


Fig. 5.8 Spin 3/2, parity 1 baryon decuplet. The I_3 axis is the abscissa, while the Y axis is the ordinate. The Ω^- has $Y = 0$, and the Σ s have $I_3 = 0$

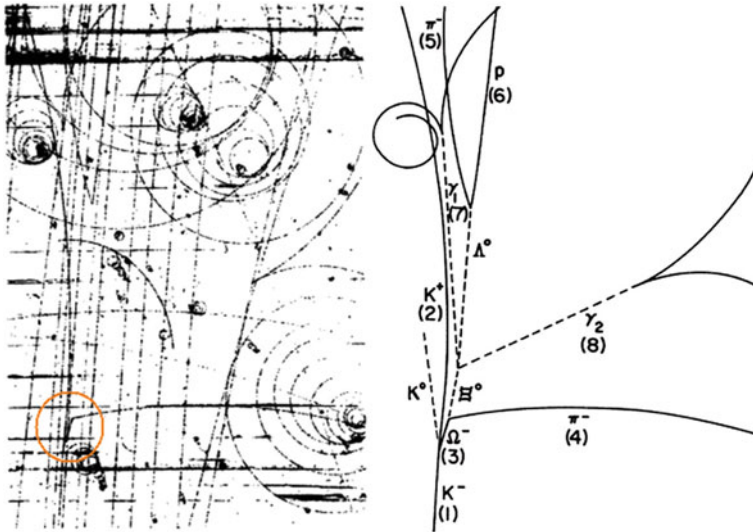
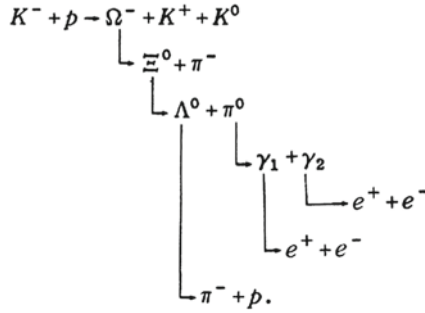


Fig. 5.9 Bubble chamber picture of the first Ω^- . From V.E. Barnes et al., “Observation of a Hyperon with Strangeness Minus Three”, Physical Review Letters 12 (1964) 204

proton in the liquid hydrogen of bubble chamber producing a K^0 , a K^+ , and a Ω^- , which then decays according to the following scheme:



Measuring the final state charged particles and applying energy–momentum conservation, the mass of the Ω^- was reconstructed with a value of $(1686 \pm 12) \text{ MeV}/c^2$, in agreement with the prediction of Gell-Mann and Ne’eman.

This “exotic” classification was thus widely accepted, but something more fundamental should be behind it!

5.4 The Quark Model

5.4.1 $SU(3)_{\text{flavor}}$

The Gell-Mann and Ne’eman meson and baryon multiplets were then recognized as representations of $SU(3)$ group symmetry but, it was soon realized, they were not the fundamental ones; they could be generated by the combination of more fundamental representations. In 1964, Gell-Mann³ and Zweig proposed as fundamental representation a triplet (3) of hypothetical spin 1/2 particles named *quarks*. Its conjugate representation ($\bar{3}$) would be the triplet of *antiquarks*. Two of the quarks (named *up*, *u*, and *down*, *d*, quarks) formed a isospin duplet and the other (named *strange*, *s*), which has strangeness quantum number different from zero, a isospin singlet. The fundamental representations of quarks and antiquarks formed triangles in the (I_3, Y) plane (Fig. 5.10).

This classification of quarks into *u*, *d*, and *s* states introduces a new symmetry called *flavor* symmetry, and the corresponding $SU(3)$ group is labeled as $SU(3)_{\text{flavor}}$ (shortly $SU(3)_f$) whenever confusion is possible with the group $SU(3)_{\text{color}}$ (shortly $SU(3)_c$) of strong interactions that will be discussed in the next chapter.

Mesons are quark–antiquark bound states, whereas baryons are composed by three quarks (antibaryons by three antiquarks). To reproduce the hadrons quantum

³Murray Gell-Mann (New York City 1929) entered the Yale university at the age of 15, and obtained his PhD from the MIT at 22. In the first part of his scientific career he gave important contributions to particle physics, in particular formulating the “quarks” hypothesis (the fanciful term was taken from Joyce’s novel *Finnegans Wake*). In a later stage he studied adaptive systems and emergent phenomena associated with complexity. He was awarded the Nobel Prize in Physics 1969 for his “discoveries concerning the classification of elementary particles and their interaction”.

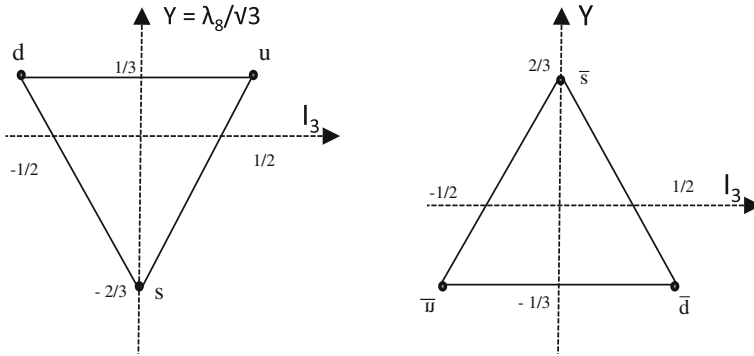


Fig. 5.10 Fundamental representations (3) and (3̄) of SU(3)

numbers, quarks must have fractional electric charge and fractional baryonic number. Their quantum numbers are as follows:

	Q	I	I_3	S	B	Y
u	$+2/3$	$1/2$	$+1/2$	0	$1/3$	$1/3$
d	$-1/3$	$1/2$	$-1/2$	0	$1/3$	$1/3$
s	$-1/3$	0	0	-1	$1/3$	$-2/3$

The mesons multiplets are obtained by the direct product of the (3) and (3̄) SU(3) representations, which gives an octet and a singlet:

$$3 \otimes \bar{3} = 8 \oplus 1. \tag{5.84}$$

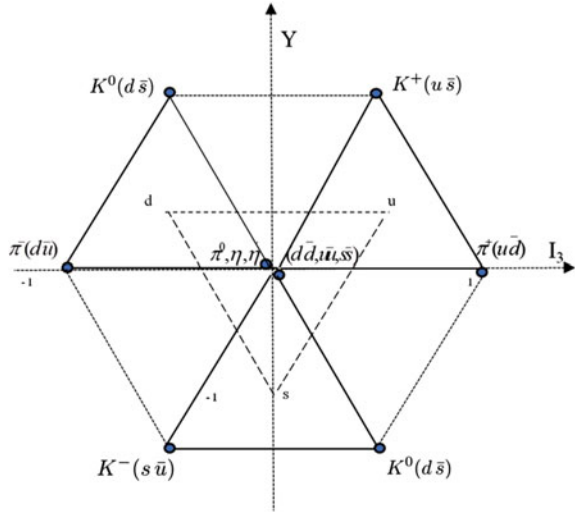
Graphically, the octet can be drawn centering in each quark vertex the inverse anti-quark triangle (Fig. 5.11).

There are three states with $I_3 = 0$ and $Y = 0$ both for pseudo-scalars (π^0, η, η') and vectors (ρ^0, ω, ϕ). The π^0 and the ρ^0 are the already well-known states with $I = 1, I_3 = 0$ ($\frac{1}{\sqrt{2}}(u\bar{u} - d\bar{d})$). The other states should then correspond to the SU(3) symmetric singlet $\frac{1}{\sqrt{3}}(u\bar{u} + d\bar{d} + s\bar{s})$, and to the octet isospin singlet, orthogonal to the SU(3) singlet, $\frac{1}{\sqrt{6}}(u\bar{u} + d\bar{d} - 2s\bar{s})$; however, the physically observed states are mixtures of these two “mathematical” singlets. Due to these mixings, there is in fact a combination of the SU(3) octet and singlet which is commonly designated as the “nonet.”

The quark content of a meson can be accessed studying its decay modes.

Baryon multiplets are obtained by the triple direct product of the (3) SU(3) representations. The 27 possible three quark combinations are then organized in a decuplet, two octets, and a singlet:

Fig. 5.11 “nonet” (octet + singlet) of pseudo-scalars mesons



$$3 \otimes 3 \otimes 3 = 10 \oplus 8 \oplus 8 \oplus 1. \tag{5.85}$$

In terms of the exchange of the quark flavor, it can be shown that the decuplet state wave functions are completely symmetric, while the singlet state wave function is completely antisymmetric. The octet state wave functions have mixed symmetry. The total wave function of each state is however not restricted to the flavor component. It must include also a spatial component (corresponding to spin and to the orbital angular momentum) and a color component which will be discussed in the next section.

5.4.2 Color

Color is at the basis of the present theory of strong interactions, QCD (see Sect. 6.4), and its introduction solves the so-called Δ^{++} puzzle. The Δ^{++} is formed by three u quarks with orbital angular momentum $l = 0$ (it is a ground state) and in the same spin projection state (the total spin is $J = 3/2$). Therefore, its flavor, spin, and orbital wave functions are symmetric, while the Pauli exclusion principle imposes that the total wave functions of states of identical fermions (as it is the case) should be antisymmetric.

In color space, quarks are represented by complex three-vectors (the generalization of the two-dimensional spinors). The number of colors in QCD is $N_c = 3$, as we shall see later in this Chapter; the quark colors are usually designated as *Red*, *Blue* and *Green*, having the antiquark the corresponding anticolors.

Quarks interact via the emission or absorption of color field bosons, the *gluons*. There are eight gluons corresponding to the eight generators of the SU(3) group (see

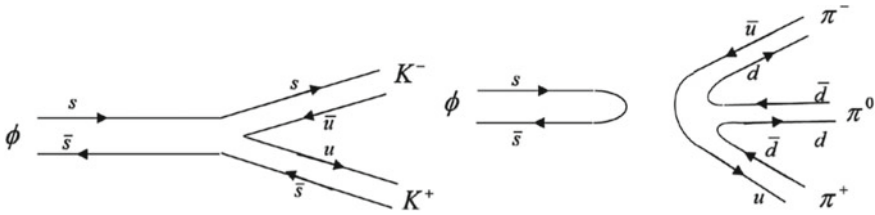


Fig. 5.12 OZI favored (left) and suppressed (right) ϕ decay diagrams

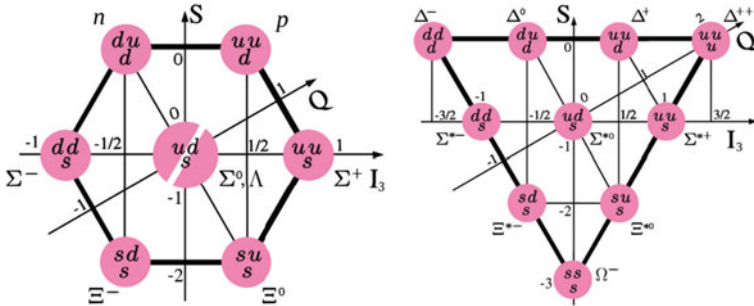


Fig. 5.13 Baryon ground states in the quark model: the spin 1/2 octet (left), and the spin 3/2 decuplet (right). The vertical (S)-axis corresponds to the Y -axis, shifted by 1 ($Y = 0$ corresponds to $S = -1$). By Trassiorf [own work, public domain], via Wikimedia Commons

Sect. 5.3.5). Gluons are in turn colored, and the emission of a gluon changes the color.

(Anti)baryons are singlet states obtained by the combination of three (anti)quarks; mesons are singlet states obtained by the combination of one quark and one antiquark. All stable hadrons are color singlets, i.e., they are neutral in color.

This is the main reason behind the so-called OZI (Okubo–Zweig–Iizuka) rule, which can be seen, for example, in the case of the ϕ the decay into a pair of kaons which is experimentally favored (86% branching ratio) in relation to the decay into three pions which however has a much larger phase space. The suppression of the 3π mode can be seen as a consequence of the fact that “decays with disconnected quark lines are suppressed” (Fig. 5.12). Being the $s\bar{s}$ state a color singlet, the initial and the final state in the right plot cannot be connected by a single gluon, being the gluon a colored object (see Sect. 6.4). Indeed, one can prove that the “disconnected” decay would need the exchange of at least three gluons.

In color space, the physical states are antisymmetric singlets (the total color charge of hadrons is zero, the strong interactions are short range, confined to the interior of hadrons and nuclei). The product of the spin wave function and the flavor wave function in ground states (angular orbital momentum = 0) must then be symmetric. The net result is that the ground-state baryons are organized in a symmetric spin 1/2 octet and in a symmetric spin 3/2 decuplet (Fig. 5.13).

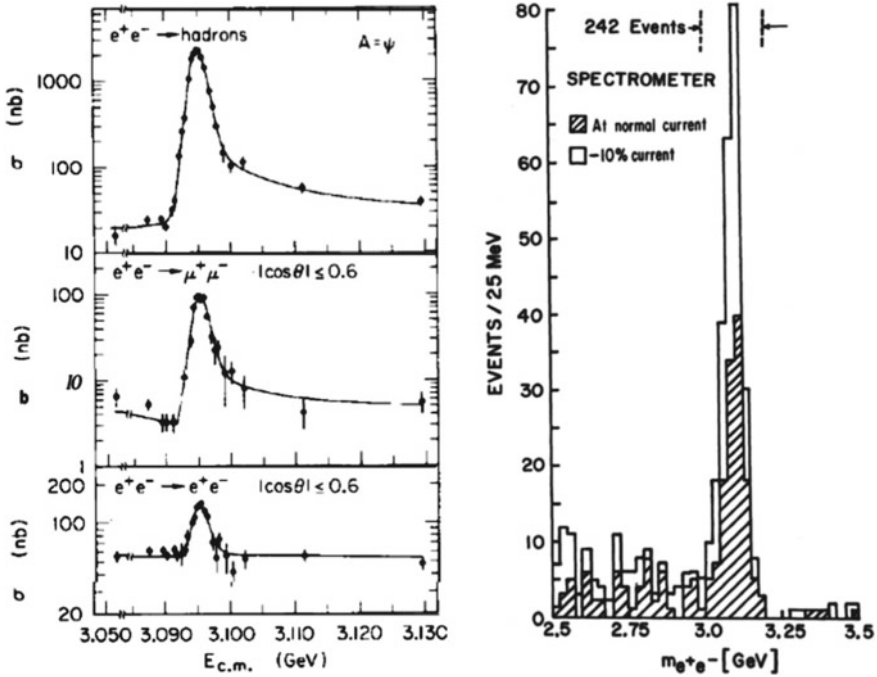


Fig. 5.14 J/ψ invariant mass plot in e^+e^- annihilations (left) and in proton–beryllium interactions (right). Credits: Nobel foundation

5.4.3 Excited States (Nonzero Angular Momenta Between Quarks)

Hundreds of excited states have been discovered with nonzero orbital angular momentum; they can be organized in successive SU(3) multiplets.

In the case of mesons, these states are labeled using the notation of atomic physics. In the case of baryons, two independent orbital angular momenta can be defined (between for instance two of the quarks, said to form a diquark state, and between this diquark and the third quark), and the picture is more complex.

5.4.4 The Charm Quark

In November 1974, there was a revolution in particle physics: the simultaneous discovery by two groups⁴ of a heavy and narrow (implying relatively long life-

⁴The Nobel Prize in Physics 1976 was awarded to Burton Richter (New York City 1931) and Samuel Ting (Ann Arbor, Michigan, 1936) “for their pioneering work in the discovery of a heavy elementary

time) resonance (Fig. 5.14). One group was led by Burton Richter and was studying electron–positron annihilations at Stanford Linear Accelerator Center (SLAC), and the other was lead by Samuel Ting and studied proton–beryllium interactions at BNL (Brookhaven National Laboratory). The BNL group named the particle “ J ,” while the SLAC group called it “ ψ ”; it was finally decided to name it “ J/ψ .” The resonance was too narrow to be an excited state—in this case, a hadronic decay would have been expected, and thus a width of $\sim 150 \text{ MeV}/c^2$.

In terms of the quark model, the J/ψ can be interpreted as a $c\bar{c}$ (where c stands for a new quark flavor, called the *charm*, which has an electric charge of $2/3$) vector (being produced in $e^+e^- \rightarrow \gamma^* \rightarrow J/\psi$) meson. The possibility of the existence of a fourth flavor was suggested in 1964 by, among others, Bjorken and Glashow for symmetry reasons: at that time, four leptons—the electron, the muon, and their respective neutrinos—were known, and just three quarks. Later, in 1970, Glashow, Iliopoulos, and Maiani demonstrated that a fourth quark was indeed needed to explain the suppression of some *neutral current* weak processes—this is the so-called GIM mechanism that will be discussed in Sect. 6.3.6.

With the existence of a fourth flavor, the flavor symmetry group changes from $SU(3)$ to $SU(4)$ giving rise to more complex multiplets which were named “supermultiplets.” Supermultiplets can be visualized (Fig. 5.15) as solids in a three-dimensional space I_3, Y, C , where C is the new charm quantum number.

A rich spectroscopy of charmed hadrons was open. For instance, the pseudo-scalar $SU(3)$ octet becomes a 15-particle $SU(4)$ multiplet with seven new mesons with at least a c quark ($D^0(c\bar{u}), D^+(c\bar{d}), D_s(c\bar{s}), \eta_c(c\bar{c}), \bar{D}^0(\bar{c}u), \bar{D}^+(\bar{c}d), \bar{D}_s(\bar{c}s)$), and the spin $3/2$ decuplet of baryons becomes a 20-particle multiplet.

5.4.4.1 Quarkonia: The Charmonium

The $c\bar{c}$ states, named *charmonium* states, are particularly interesting; they correspond to nonrelativistic particle/antiparticle bound states. Charmonium states have thus a structure of excited states similar to positronium (an e^+e^- bound state), but their energy levels can be explained by a potential in which a linear term is added to the Coulomb-like potential, which ensures that an infinite energy is needed to separate the quark and the antiquark (no free quarks have been observed up to now, and we found a clever explanation for this fact, as we shall see):

particle of a new kind”. Richter graduated from Far Rockaway High School, that also educated Richard Feynman; he became a professor at Stanford and later director of the Stanford Linear Accelerator Center. Ting was educated in China and Taiwan and returned to US for attending the University of Michigan, becoming later staff member of CERN and professor at the Massachusetts Institute of Technology (MIT). In the second part of his career Ting moved to astroparticle physics, and he is now the lead proposer and Principal Investigator of the AMS experiment (see Chap. 10). The Japanese K. Niu and collaborators had already published candidates for charm (no such name was ascribed to this new quark at that time) in a cosmic ray experiment using nuclear emulsions in 1971. These results, taken seriously in Japan, were not accepted as evidence for the discovery of charm by the majority of the US and European scientific communities. Once again, cosmic ray physics was the pathfinder.

$$V(r) \simeq -\frac{4}{3} \frac{\alpha_s}{r} + \kappa r, \tag{5.86}$$

where r is the radius of the bound state, α_s is the equivalent for the strong interactions of the fine structure constant α , κ is a positive constant, and the coefficient $4/3$ has to do with the color structure of strong interactions; we shall discuss it in larger detail in Sect. 6.4.6.

The linear term dominates for large distances. Whenever the pair is stretched, a field string is formed storing potential energy; at some point, (part of) the stored energy can be converted, by tunnel effect, into mass and a new quark–antiquark pair can be created transforming the original meson into two new mesons (Fig. 5.16). This process is named quark hadronization and plays a central role in high-energy hadronic interactions.

In positronium spectroscopy, one can obtain the energy levels by solving the Schrödinger equation with a potential $V_{em} = -\alpha/r$; the result is

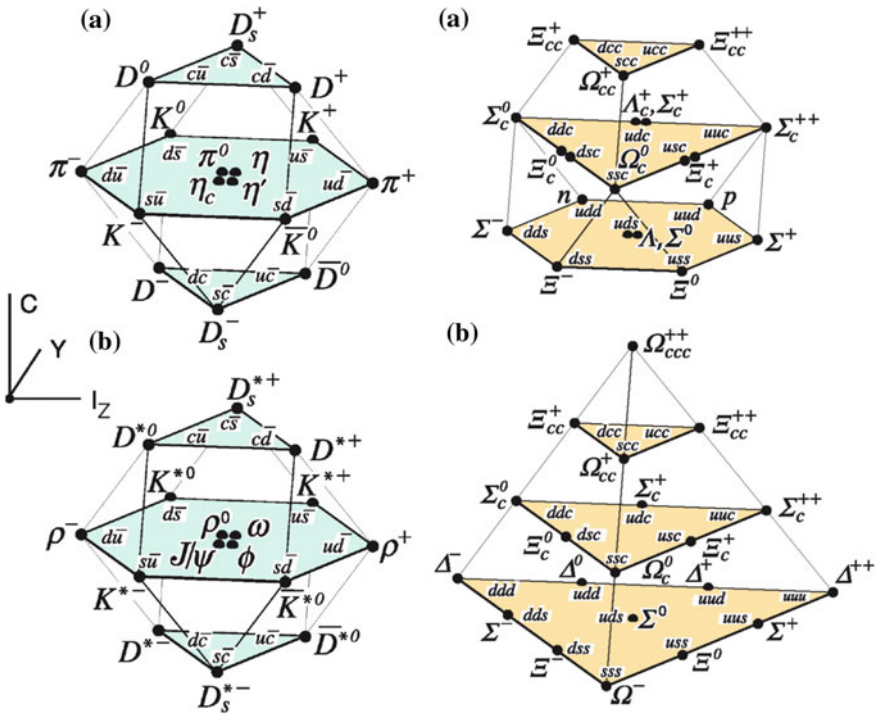


Fig. 5.15 Left: 16-plets for the pseudo-scalar (a) and vector (b) mesons made of the u , d , s , and c quarks as a function of isospin I_3 , charm C , and hypercharge $Y = B + S + C$. The nonets of light mesons occupy the central planes to which the $c\bar{c}$ states have been added. Right: SU(4) multiplets of baryons made of u , d , s , and c quarks: (a) The 20-plets including an SU(3) octet; (b) The 20-plets with an SU(3) decuplet. From K.A. Olive et al. (Particle Data Group), Chin. Phys. C 38 (2014) 090001

$$E_{p;n} = -\frac{\alpha m_e c^2}{4n^2}.$$

Note that these levels are approximately equal to the energy levels of the hydrogen atom, divided by two: this is due to the fact that the mass entering in the Schrödinger equation is the *reduced* mass m_r of the system, which in the case of hydrogen is approximately equal to the electron mass ($m_r = m_e m_p / (m_e + m_p)$), while in the case of positronium, it is exactly $m_e/2$. The spin-orbit interaction splits the energy levels (fine splitting), and a further splitting (hyperfine splitting) is provided by the spin-spin interactions.

The left plot of Fig. 5.17 shows the energy levels of positronium. They are indicated by the symbols $n^{2S+1}L_s$ (n is the principal quantum number, S is the total spin, L indicates the orbital angular momentum in the spectroscopic notation (S being the $\ell = 0$ state), and s is the spin projection).

The right plot of Fig. 5.17 shows the energy levels of charmonium; they can be obtained inserting the potential (5.86) into the Schrödinger equation. One obtains $\kappa \sim 1 \text{ GeV/fm}$, and $\alpha_s \sim 0.3$.

Fig. 5.16 Hadronization: the string mechanism

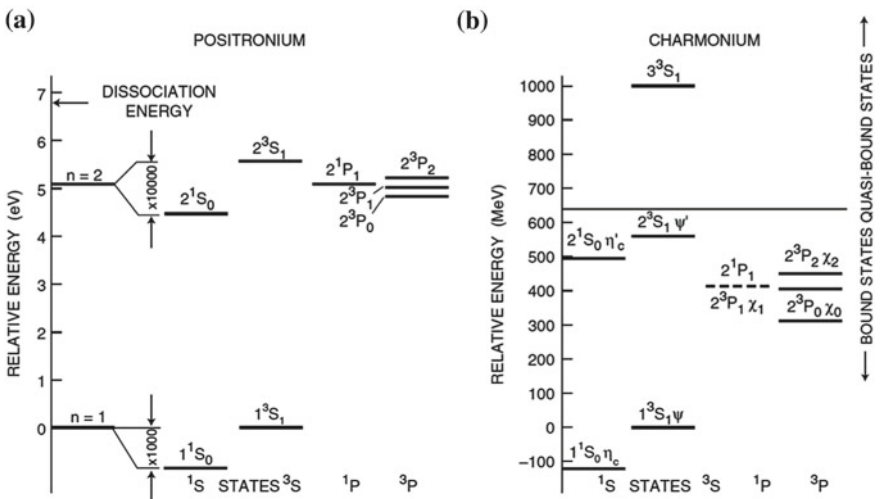
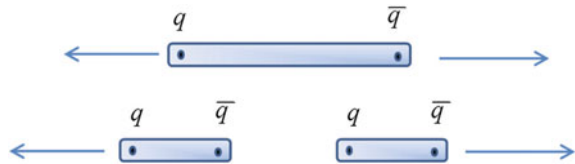


Fig. 5.17 Energy levels for (a) the positronium and (b) the charmonium states. From S. Braibant, G. Giacomelli, and M. Spurio, “Particles and fundamental interactions,” Springer 2012

The bottom quark, which will be introduced in the next section, has an even larger mass, and it gives rise to a similar spectroscopy of quarkonia.

5.4.5 *Beauty and Top*

A fifth quark was discovered a few years later. In 1977, an experiment in Fermilab led by Leon Lederman studied the mass spectrum of $\mu^-\mu^+$ pairs produced in the interaction of a 400 GeV proton beam on copper and platinum targets. A new heavy and narrow resonance, named the Υ , was found, with a mass of around $9.46 \text{ GeV}/c^2$.

The Υ was interpreted as a $b\bar{b}$ vector meson where b stands for a new quark flavor, the *bottom* or *beauty*, which has, like the d and the s , an electric charge of $-1/3$. Several hadrons containing at least a b quark were discovered. A family of $b\bar{b}$ mesons, called the bottomium and indicated by the letter Υ , was there, as well as mesons and baryons resulting from the combination of b quarks with lighter quarks: pseudo-scalar mesons like the B^+ ($u\bar{b}$), B_c^+ ($c\bar{b}$), the B^0 ($d\bar{b}$), and the B_s^0 ($s\bar{b}$); bottom baryons like Λ_b^0 (udb), Ξ_b^0 (usb), Ξ_b^- (dsb), Ω_b^- (ssb). Heavy mesons and baryons with a single heavy quark are very interesting. The light quarks surround the heavy quark in a strong force analogy of electrons around the proton in the electromagnetically bound hydrogen atom.

The discovery of the b quark inaugurated a third generation or family of quarks. Each family is formed by two quarks, one with electric charge $+2/3$ and the other with electric charge $-1/3$ (the first family is formed by quarks u and d ; the second by quarks c and s). In the lepton sector, as will be discussed at the end of this chapter, there were at that time already five known leptons (the electron, the muon, their corresponding neutrinos, and a recently discovered heavy charged lepton, the tau). With the bottom quark, the symmetry was restored between quarks and leptons but the sixth partners both in the quark and in lepton (the tau neutrino) sector were missing. The existence of a third family of quarks had indeed been predicted already in 1973, before the discovery of the J/ψ , by Makoto Kobayashi and Toshihide Maskawa, to accommodate in the quark model the CP violation observed in the $K^0\bar{K}^0$ system (this will be discussed in Chap. 6). The hypothetical sixth quark was named before its discovery the “top” quark.

The top quark was missing and for many years, and many people looked for it in many laboratories (in the USA and in Germany, Japan, CERN), both at electron–positron and at proton–(anti)proton colliders. A strong indication of a top with a mass around $40 \text{ GeV}/c^2$ was even announced in 1984 but soon dismissed. Lower limits on the top mass were later established, and indications on the value of the mass were derived from the standard model (see Chap. 7); finally, in 1995, the discovery of the top quark was published by the CDF experiment (and soon after by the D0 experiment) at Fermilab, at a mass of $(176 \pm 18) \text{ GeV}/c^2$. The present (2018) world average of the direct measurements is $(173.1 \pm 0.6) \text{ GeV}/c^2$. The top is heavier than a gold nucleus; with such a large mass, its decay phase space is huge and its lifetime is very

short, even if the decay is mediated by the weak force. It is so short (the estimated value is around 5×10^{-25} s) that the top does not live long enough to hadronize: there are no top hadrons.

5.4.6 Exotic Hadrons

It is evident that it is possible to form other color singlet bound states than the ordinary mesons ($q\bar{q}$) and baryons (qqq). Indeed many states are predicted formed by: just gluons (glueballs); two quarks and two antiquarks (tetraquarks); four quarks and one antiquark (pentaquarks); or six quarks (hexaquarks). These hadrons had been searched for long and many candidates did exist, but only recently (2014 and 2015) the LHCb collaboration at CERN confirmed the existence of a tetraquark (the $Z(4430)$, a bound $c\bar{c}d\bar{u}$ state) and two pentaquarks (the $P_c^+(4380)$ and the $P_c^+(4450)$, both bound $uudc\bar{c}$ states). A rich spectroscopy can be studied in the future.

5.4.7 Quark Families

At present six quark flavors (u, d, c, s, t, b) are known, and they can be organized into three families:

$$\begin{pmatrix} u \\ d \end{pmatrix} \begin{pmatrix} c \\ s \end{pmatrix} \begin{pmatrix} t \\ b \end{pmatrix}.$$

Their masses cover an enormous range, from the tens of MeV/c^2 for the u and the d quarks,⁵ to the almost $200 \text{ GeV}/c^2$ for the t quark. The flavor symmetry that was the clue to organize the many discovered hadrons is strongly violated. Why? Is there a fourth, a fifth (. . .), family to be discovered? Are quarks really elementary? These are questions we hope to answer during this century.

5.5 Quarks and Partons

In the words of Murray Gell-Mann in 1967, quarks seemed to be just *mathematical entities*. This picture was deeply changed in a few years by the results of deep inelastic scattering experiments.

⁵The problem of the determination of the quark masses is not trivial. We can define as a “current” quark mass the mass entering in the Lagrangian (or Hamiltonian) representation of a hadron; this comes out to be of the order of some MeV/c^2 for u, d quarks, and $\sim 0.2 \text{ GeV}/c^2$ for s quarks. However, the strong field surrounds the quarks in such a way that they acquire a “constituent” (effective) mass including the equivalent of the color field; this comes out to be of the order of some $300 \text{ MeV}/c^2$ for u, d quarks, and $\sim 0.5 \text{ GeV}/c^2$ for s quarks. Current quark masses are almost the same as constituent quark mass for heavy quarks.

Indeed in the 1950s Robert Hofstadter,⁶ in a series of Rutherford-like experiments using a beam of electrons instead of α particles (electrons have no strong interactions), showed departures from the expected elastic point cross section. Nucleons (protons and neutrons) are not point-like particles. The proton must have a structure and the quarks could be thought as its constituents.

5.5.1 Elastic Scattering

The electron–proton elastic cross section, approximating the target proton as a point-like spin 1/2 particle with a mass m_p , was calculated by Rosenbluth (Sect. 6.2.8):

$$\frac{d\sigma}{d\Omega} = \frac{\alpha^2 \cos^2\left(\frac{\theta}{2}\right)}{4E^2 \sin^4\left(\frac{\theta}{2}\right)} \frac{E'}{E} \left[1 + \frac{Q^2}{2m_p^2} \tan^2\left(\frac{\theta}{2}\right) \right] \quad (5.87)$$

where the first factor is the Mott cross section (scattering of an electron in a Coulomb field, see Chap. 2); the second (E'/E) takes into account the energy lost in the recoil of the proton; and the third factor is the spin/spin interaction. Note that for a given energy of the incident electron there is just one independent variable, which is usually chosen by experimentalists to be the scattering angle, θ . In fact, the energy of the scattered electron, E' , can be expressed as a function of θ as

$$E' = \frac{E}{1 + E(1 - \cos \theta)/m_p}. \quad (5.88)$$

The measured cross section had however a stronger Q^2 dependence as would be expected in the case of a finite size proton. This cross section was parameterized as:

$$\frac{d\sigma}{d\Omega} = \frac{\alpha^2 \cos^2\left(\frac{\theta}{2}\right)}{4E^2 \sin^4\left(\frac{\theta}{2}\right)} \frac{E'}{E} \left[\frac{G_E^2(Q^2) + \frac{Q^2}{4m_p^2} G_M^2(Q^2)}{1 + \frac{Q^2}{4m_p^2}} + 2 \frac{Q^2}{4m_p^2} G_M^2(Q^2) \tan^2\left(\frac{\theta}{2}\right) \right] \quad (5.89)$$

where $G_E^2(Q^2)$ and $G_M^2(Q^2)$ are called, respectively, the electric and the magnetic form factors (if $G_E = G_M = 1$, the Rosenbluth formula (5.87) is recovered).

⁶Robert Hofstadter (1915–1990) was an American physicist. He was awarded the 1961 Nobel Prize in Physics “for his pioneering studies of electron scattering in atomic nuclei and for his consequent discoveries concerning the structure of nucleons.” He worked at Princeton before joining Stanford University, where he taught from 1950 to 1985. In 1948, Hofstadter patented the thallium activated NaI gamma-ray detector, still one of the most used radiation detectors. He coined the name “fermi,” symbol fm, for the scale of 10^{-15} m. During his last years, Hofstadter became interested in astrophysics and participated to the design of the EGRET gamma-ray space telescope (see Chap. 10).

At low Q^2 , $G_E(Q^2)$ and $G_M(Q^2)$ can be interpreted as the Fourier transforms of the electric charge and of the magnetization current density inside the proton. In the limit $Q^2 \rightarrow 0$ ($\lambda \rightarrow \infty$ for the exchanged virtual photon), the electron “sees” the entire proton and it could be expected that $G_E(0) = G_M(0) = 1$. This is what the experiment tells for G_E , but it is not the case for G_M . In fact, the measured value is $G_M(0) = \mu_p \simeq 2.79$. The proton has an anomalous magnetic moment μ_p which reveals already that the proton is not a Dirac point-like particle. The same is observed for the neutron which has $\mu_n \simeq -1.91$.

In fact, at low Q^2 ($Q^2 < 1 - 2 \text{ GeV}^2$), the experimental data on G_E and G_M are well described by the dipole formula

$$G_E(Q^2) \simeq \frac{G_M(Q^2)}{\mu_p} \simeq \left(\frac{1}{1 + Q^2/0.71 \text{ GeV}^2} \right)^2 \quad (5.90)$$

suggesting similar spatial distributions for charges and currents. However, recent data at higher Q^2 using polarized beams showed a much richer picture reflecting a complex structure of constituents and their interactions.

5.5.2 Inelastic Scattering Kinematics

The scattering of an electron on a proton may, if the electron energy is high enough, show the substructure of the proton. At first order, such scattering (Fig. 5.18) can be seen as the exchange of a virtual photon (γ^*) with four-momentum:

$$q = (p_1 - p_3) = (p_4 - p_2), \quad (5.91)$$

where p_1 and p_3 are, respectively, the four-momentum of the incoming and outgoing electron, p_2 is the target four-momentum, and p_4 is the four-momentum of the final hadronic state which has an invariant mass $M = \sqrt{p_4^2}$ (see Fig. 5.18). In case of elastic scattering, $M = m_p$.

The square of the exchanged four-vector is then

$$q^2 = -Q^2 = (p_1 - p_3)^2 = (p_4 - p_2)^2. \quad (5.92)$$

In the laboratory reference frame:

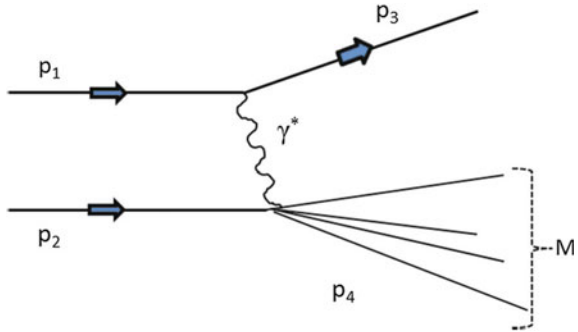
$$p_1 = (E, \mathbf{K}); p_2 = (m_p, 0); p_3 = (E', \mathbf{K}'); p_4 = \left(\sqrt{M^2 + \mathbf{p}_4^2}, \mathbf{p}_4 \right). \quad (5.93)$$

The center-of-mass energy is, as it was seen in Chap. 2, the square root of the Mandelstam variable s :

$$s = (p_1 + p_2)^2, \quad (5.94)$$

which in the laboratory reference frame is given (neglecting $m_e^2 \sim 0$) by:

Fig. 5.18 Deep inelastic scattering kinematics



$$s \simeq m_p(2E + m_p). \tag{5.95}$$

It is also useful to construct other Lorentz invariant variables defined through internal products of the above four-vectors:

- the lost energy ν

$$\nu = \frac{qp_2}{m_p}. \tag{5.96}$$

ν in the laboratory reference frame is the energy lost by the electron:

$$\nu = E - E'; \tag{5.97}$$

- the inelasticity y

$$y = \frac{qp_2}{p_1 p_2}. \tag{5.98}$$

y is dimensionless, and it is limited to the interval $0 \leq y \leq 1$. In the laboratory frame is the fraction of the energy lost by the electron:

$$y = \frac{\nu}{E}; \tag{5.99}$$

- the Bjorken variable, x

$$x = \frac{Q^2}{2p_2 q}, \tag{5.100}$$

x is also dimensionless and limited to the interval $0 \leq x \leq 1$. Using the definition of ν , x can also be expressed as:

$$x = \frac{Q^2}{2m_p \nu}, \tag{5.101}$$

or imposing energy and momentum conservation at the hadronic vertex:

$$x = \frac{Q^2}{Q^2 + M^2 - m_p^2}. \quad (5.102)$$

If $x = 1$ then $M = m_p$, the elastic scattering formula is recovered.

At a fixed center-of-mass energy, \sqrt{s} , the inelastic scattering final state can be characterized by the Lorentz invariant variables, Q^2 , M^2 , x , y , as well as by the scattered electron energy E' and scattered angle θ in the laboratory reference frame. However, from all those variables, only two are independent. The experimental choice is usually the directly measured variables E' and θ , while the theoretical interpretation is usually done in terms of Q^2 and ν or Q^2 and x .

Many relations can be built connecting all these variables. The following are particularly useful:

$$Q^2 \simeq 4EE' \sin^2 \left(\frac{\theta}{2} \right); \quad (5.103)$$

$$Q^2 \simeq 2M\nu; \quad (5.104)$$

$$Q^2 = xy(s - m_p^2); \quad (5.105)$$

$$M^2 = m_p^2 + 2m_p\nu - Q^2. \quad (5.106)$$

5.5.3 Deep Inelastic Scattering

The differential electron–proton inelastic cross section is parameterized, similarly to what was done in the case of the electron–proton elastic cross section, introducing two independent functions. These functions, called the structure functions W_1 and W_2 , can be expressed as a function of any two of the kinematic variables discussed in the previous section. Hereafter, the choice will be Q^2 and ν . Hence,

$$\frac{d\sigma}{d\Omega dE'} = \frac{\alpha^2 \cos^2 \left(\frac{\theta}{2} \right)}{4 E^2 \sin^4 \left(\frac{\theta}{2} \right)} \frac{E'}{E} \left[W_2(Q^2, \nu) + 2W_1(Q^2, \nu) \tan^2 \left(\frac{\theta}{2} \right) \right]. \quad (5.107)$$

$W_1(Q^2, \nu)$ describes the interaction between the electron and the proton magnetic moments and can be neglected for low Q^2 .

In the limit of electron–proton elastic scattering ($x \rightarrow 1$, $\nu = Q^2/2m_p$), these structure functions should reproduce the elastic cross section formula discussed above:

$$W_1(Q^2, \nu) = \frac{Q^2}{4m_p^2} G_M^2(Q^2) \delta \left(\nu - \frac{Q^2}{2m_p} \right); \quad (5.108)$$

$$W_2(Q^2, \nu) = \frac{G_E^2(Q^2) + \frac{Q^2}{4m_p^2} G_M^2(Q^2)}{1 + \frac{Q^2}{4m_p^2}} \delta \left(\nu - \frac{Q^2}{2m_p} \right). \quad (5.109)$$

If $G_E = G_M = 1$ (elastic scattering of electrons on a point 1/2 spin particle with mass m_p and charge e) the Rosenbluth formula (5.87) is recovered and:

$$W_1(Q^2, \nu) = \frac{Q^2}{4m_p^2} \delta\left(\nu - \frac{Q^2}{2m_p}\right); \quad W_2(Q^2, \nu) = \delta\left(\nu - \frac{Q^2}{2m_p}\right). \quad (5.110)$$

The difference between scattering on point-like or finite size particles is thus translated into the form factors G_E and G_M . In the case of a scattering over point-like particles, the exchanged virtual photon “sees” always the same charge whatever the Q^2 . In the case of a finite size particle, the photon wavelength ($\lambda \sim 1/\sqrt{Q^2}$) limits the *observed* volume inside the target. For smooth charge distributions inside the target, it is therefore trivial to predict that when $Q^2 \rightarrow \infty$:

$$W_1(Q^2, \nu) \rightarrow 0; \quad W_2(Q^2, \nu) \rightarrow 0.$$

On the contrary, if the charge distribution is “concentrated” in a few space points, some kind of point-like behavior may be recovered. Such behavior was predicted by James Bjorken in 1967 who postulated, for high Q^2 and ν , the scaling of the structure functions:

$$W_1(Q^2, \nu) \rightarrow \frac{1}{m_p} F_1(w); \quad W_2(Q^2, \nu) \rightarrow \frac{1}{\nu} F_2(w) \quad (5.111)$$

where w , the Bjorken scaling variable, is the inverse of the x variable:

$$w = \frac{1}{x} = \frac{2m_p \nu}{Q^2}. \quad (5.112)$$

According to the above definitions, F_1 and F_2 are dimensionless functions, while W_1 and W_2 have dimensions E^{-1} .

While Bjorken was suggesting the scaling hypothesis, the groups lead by J. Friedman, H. Kendall, and R. Taylor⁷ designed and built at SLAC electron spectrometers able to measure energies up to 20 GeV for different scattering angles. The strong Q^2 dependence of the elastic form factors was then confirmed up to $Q^2 \simeq 30 \text{ GeV}^2$ while, surprisingly, in the region $M > 2 \text{ GeV}$, the inelastic cross section showed a very mild Q^2 dependence (Fig. 5.19, left).

On the other hand, the $W_2(Q^2, \nu)$ structure function showed, at these relative small energies, already an approximate Bjorken scaling. In fact, $F_2(w) = \nu W_2(Q^2, \nu)$ was found to be a universal function of $w = 1/x$ as demonstrated by measurements at different energies and angles of the scattered particle (Fig. 5.19, right) or at different Q^2 but keeping w constant (Fig. 5.20).

⁷The Nobel Prize in Physics 1990 was assigned to Jerome I. Friedman, Henry W. Kendall, and Richard E. Taylor “for their pioneering investigations concerning deep inelastic scattering of electrons on protons and bound neutrons, which have been of essential importance for the development of the quark model in particle physics.”

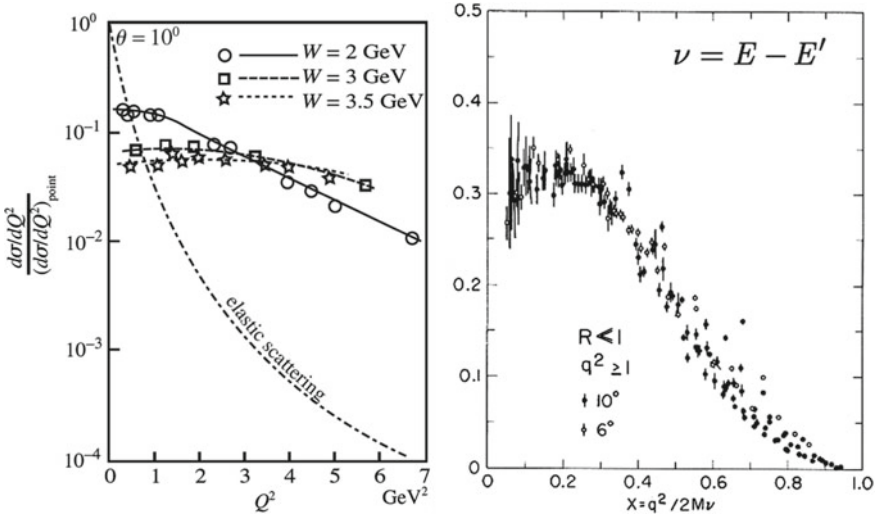
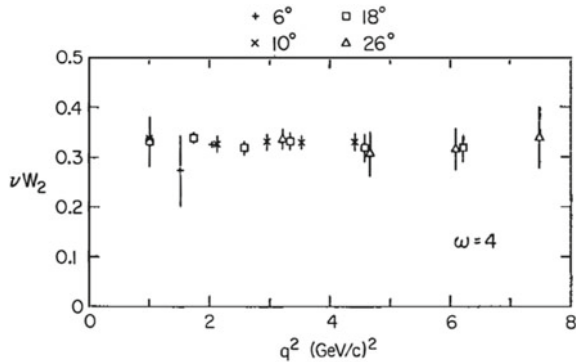


Fig. 5.19 Left: Deep inelastic electron–proton differential cross section normalized to the Mott cross section, as measured by SLAC. From Ref. [F5.2] in the “Further readings.” Adapted from Nobel Foundation, 1990. Right: νW_2 scaling: measurements at different scattered energies and angles. From W. Atwood, “Lepton Nucleon Scattering,” Proc. 1979 SLAC Summer Institute (SLAC-R-224)

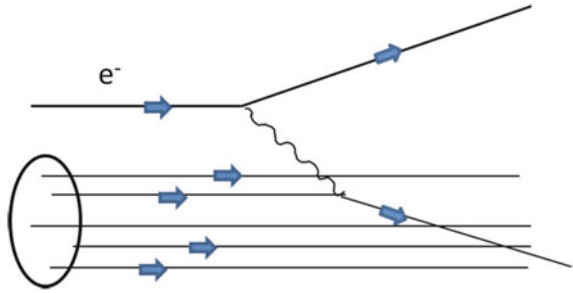
Fig. 5.20 νW_2 scaling for the proton: measurements at fixed x and at different Q^2 . From J.I. Friedman and H.W. Kendall, Annual Rev. Nucl. Science 22 (1972) 203



In 1968 Richard Feynman, just a few months after the presentation of the SLAC results, worked out a simple and elegant model which could explain these results: the electron–nucleon scattering at high energy might be seen as the scattering of the electron into free point-like charged particles in the nucleon, the *partons* (Fig. 5.21). This is the so-called quark–parton model (QPM).

The Feynman partons were soon after identified as the Gell-Mann and Ne’eman quarks. However, nowadays, the term “parton” is used often to denominate all the nucleon constituents, i.e., the quarks and antiquarks and even the gluons.

Fig. 5.21 Representation of electron–parton scattering in Feynman’s Quark–Parton Model



5.5.4 The Quark–Parton Model

In the Feynman model the partons are basically free inside the hadrons but confined in them, nobody has ever observed a parton out of one hadron. In a first approximation, the transverse momentum of the partons may be neglected and each parton may then share a fraction Z_i of the nucleon momentum and energy:

$$E_i = Z_i E ; \mathbf{p}_i = Z_i \mathbf{p} . \tag{5.113}$$

In this hypothesis the parton mass is also a fraction Z_i of the nucleon mass m_N :

$$m_i = Z_i m_N . \tag{5.114}$$

These assumptions are exact in a frame where the parton reverses its linear momentum keeping constant its energy (collision against a “wall”). In such frame (called the Breit frame, or also the infinitum momentum frame), the energy of the virtual photon is zero ($q_{\gamma^*} = (0, 0, 0, -Q)$) and the proton moves with a very high momentum toward the photon. However, even if the parton model was built in such an extreme frame, its results are valid whenever $Q^2 \gg m_N$.

Remembering the previous section, the elastic form factor of the scattering electron on a point-like spin $1/2$ particle with electric charge e_i and mass m_i can be written as

$$W_1(Q^2, \nu) = \frac{Q^2}{4m_i^2} e_i^2 \delta\left(\nu - \frac{Q^2}{2m_i}\right) ; W_2(Q^2, \nu) = e_i^2 \delta\left(\nu - \frac{Q^2}{2m_i}\right) . \tag{5.115}$$

Using the property of the δ function: $\delta(ax) = \frac{1}{|a|} \delta(x)$, and remembering that $m_i = Z_i m_N$ and $x = \frac{Q^2}{2m_N \nu}$, the electron–parton form factors are:

$$W_1(Q^2, \nu) = e_i^2 \frac{x}{2m_N Z_i} \delta(Z_i - x) ; W_2(Q^2, \nu) = e_i^2 \frac{Z_i}{\nu} \delta(Z_i - x) , \tag{5.116}$$

or, in terms of F_1 and F_2 :

$$F_1(Q^2, \nu) = e_i^2 \frac{x}{2Z_i} \delta(Z_i - x) ; F_2(Q^2, \nu) = e_i^2 Z_i \delta(Z_i - x) . \quad (5.117)$$

The δ function imposes that $Z_i \equiv x$. That means that, to comply with the elastic kinematics constraints, the exchanged virtual photon has to pick up a parton with precisely a fraction x of the nucleon momentum.

Inside the nucleon there are, in this model, partons carrying different fractions of the total momentum. Let us then define as $f_i(Z_i)$ the density probability function to find a parton carrying a fraction of momentum Z_i . The electron–nucleon form factors are thus obtained integrating over all the entire Z_i range and summing up all the partons:

$$F_1(Q^2, x) = \sum_i \int_0^1 e_i^2 \frac{x}{2Z_i} f_i(Z_i) \delta(Z_i - x) dZ_i = \sum_i e_i^2 \frac{1}{2} f_i(x) \quad (5.118)$$

and

$$F_2(Q^2, x) = \sum_i \int_0^1 e_i^2 Z_i f_i(Z_i) \delta(Z_i - x) dZ_i = x \sum_i e_i^2 f_i(x) . \quad (5.119)$$

The functions $f_i(x)$ are called the *parton density functions* (PDFs).

Comparing F_1 and F_2 , the so-called Callan–Gross relation is established:

$$F_2(Q^2, \nu) = 2x F_1(Q^2, \nu) . \quad (5.120)$$

This relation derives directly from the assumption that partons are spin 1/2 particles (if their spin would be 0 then $F_1(Q^2, \nu) = 0$) and was well verified experimentally (Fig. 5.22).

The sum of all parton momentum fractions should be 1, if the partons (quarks) were the only constituents of the nucleon:

Fig. 5.22 Validation of the Callan–Gross relation. Adapted from S. Braibant, G. Giacomelli and M. Spurio, “Particles and fundamental interactions,” Springer 2012

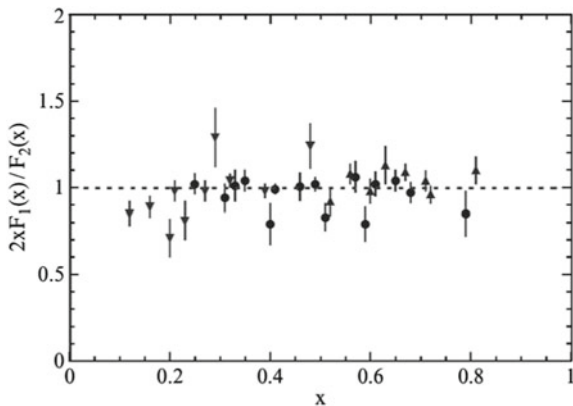
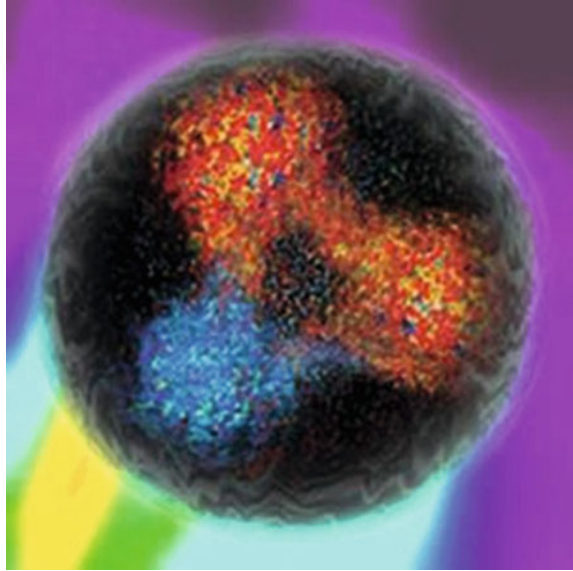


Fig. 5.23 Artistic picture of a nucleon. From <http://hendrix2.uoregon.edu/~imamura>



$$\sum_i \int_0^1 e_i^2 f_i(x) dx = 1.$$

Experimentally, however, the charged constituents of the nucleon carry only around 50 % of the total nucleon momentum. The rest of the momentum is carried by neutral particles, the gluons, which are, as it will be discussed in the next chapter, the bosons associated with the strong field that holds together the nucleon.

The real picture is more complex: instead of just three quarks, inside the nucleon there are an infinite number of quarks and antiquarks. In fact, as in the case of the electromagnetic field, where electron–positron pairs can be created even in the vacuum (the Casimir effect being a spectacular demonstration), virtual quark–antiquark pairs can be created inside the nucleon. These pairs are formed in timescales allowed by the Heisenberg uncertainties relations. In an artistic picture (Fig. 5.23), the nucleon is formed by three quarks which determine the nucleon quantum numbers and carry a large fraction of the nucleon momentum (the *valence quarks*) surrounded by clouds of virtual quark–antiquark pairs (the “sea” quarks) and everything is embedded in a background of strong field bosons (gluons).

Quarks in hadrons may have different flavors and thus different charges and masses. The corresponding PDFs are denominated according to the corresponding flavor: $u(x)$, $d(x)$, $s(x)$, $c(x)$, $b(x)$, $t(x)$ for quarks; $\bar{u}(x)$, $\bar{d}(x)$, $\bar{s}(x)$, ... for antiquarks.

The form factor F_2 for the electron–proton scattering can now, for instance, be written as a function of the specific quarks PDFs:

$$F_2^{ep}(Q^2, x) \simeq x \left[\frac{4}{9} (u(x) + \bar{u}(x)) + \frac{1}{9} (d(x) + \bar{d}(x) + s(x) + \bar{s}(x)) \right]. \quad (5.121)$$

The small contributions from heavier quarks and antiquarks can be usually neglected (due to their large masses, they are strongly suppressed). The PDFs can still be divided into valence and sea. To specify if a given quark PDF refers to valence or sea, a subscript V or S is used. For instance, the total u quark proton PDF is the sum of two PDFs:

$$u(x) = u_V(x) + u_S(x). \quad (5.122)$$

For the \bar{u} antiquark PDF, we should remember that in the proton there are no valence antiquarks, just sea antiquarks. Moreover, as the sea quarks and antiquarks appear in pairs, the sea quarks and antiquarks PDFs with the same flavor should be similar. Therefore, the \bar{u} component in the proton can be expressed as

$$\bar{u}(x) = \bar{u}_S(x) = u_S(x). \quad (5.123)$$

There are thus several new functions (the specific quarks PDFs) to be determined from the data. A large program of experiments has been carried out and in particular deep inelastic scattering experiments with electron, muon, neutrino, and antineutrino beams. The use of neutrinos and antineutrinos is particularly interesting since, as it will be discussed in the next chapter, their interactions with quarks arises through the weak force and having a well-defined helicity (neutrinos have left helicity, antineutrinos right helicity) they “choose” between quarks and antiquarks (see Sect. 6.3.4). The results of all experiments are globally analyzed and PDFs for quarks but also for gluons ($g(x)$), are obtained. At low x , the PDFs of sea quarks and gluons behave as $1/x$, and therefore their number inside the proton becomes extremely large at $x \rightarrow 0$. However, the physical observable $xf(x)$ (the carried momentum) are better behaved (Fig. 5.24).

The valence quark PDFs can then be obtained subtracting the relevant quark and antiquark PDFs:

$$u_V(x) = u(x) - \bar{u}(x); \quad d_V(x) = d(x) - \bar{d}(x). \quad (5.124)$$

Their integration over the full x range is consistent with the quark model. In fact for the proton,

$$\int_0^1 u_V(x) dx \simeq 2; \quad \int_0^1 d_V(x) dx \simeq 1. \quad (5.125)$$

The $xu_V(x)$ and $xd_V(x)$ distributions have a maximum around $1/3$ as expected but the sum of the momenta carried out by the valence quarks is (as it was discussed before) smaller than the total momentum:

$$\int_0^1 xu_V(x) dx \simeq 0.36; \quad \int_0^1 xd_V(x) dx \simeq 0.18. \quad (5.126)$$

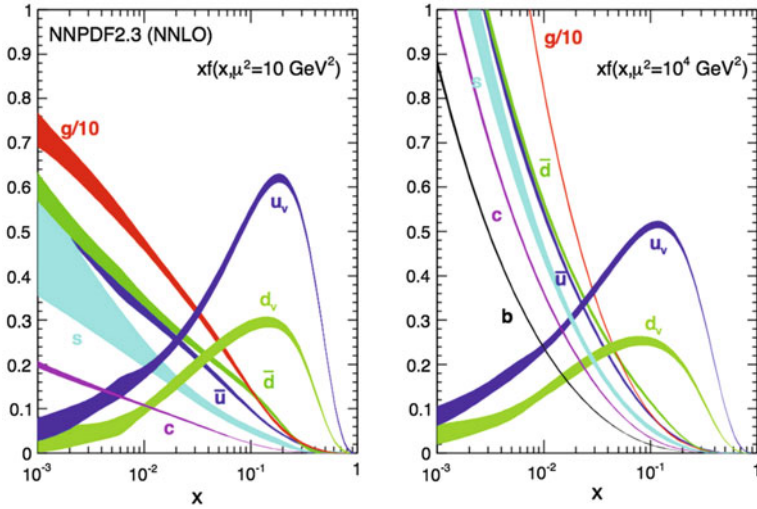


Fig. 5.24 Parton distribution functions at $Q^2 = 10 \text{ GeV}^2$ (left) and $Q^2 = 10000 \text{ GeV}^2$ (right). The gluon and sea distributions are scaled down by a factor of 10. The experimental, model, and parameterization uncertainties are shown. From K.A. Olive et al. (Particle Data Group), Chin. Phys. C 38 (2014) 090001

Many tests can be done by combining the measured form factors. An interesting quantity, for instance, is the difference of the form factor functions F_2 for electron–proton and electron–neutron scattering.

Assuming isospin invariance:

$$u^p(x) = d^n(x) ; d^p(x) = u^n(x)$$

$$\bar{u}^p(x) = \bar{u}^n(x) = \bar{d}^p(x) = \bar{d}^n(x)$$

$$s^p(x) = \bar{s}^p(x) = s^n(x) = \bar{s}^n(x) .$$

Then

$$F_2^{ep}(Q^2, x) \simeq x \left[\frac{4}{9}u_v^p(x) + \frac{1}{9}d_v^p(x) + \frac{10}{9}\bar{u}^p(x) + \frac{2}{9}\bar{s}^p(x) \right] \quad (5.127)$$

$$F_2^{en}(Q^2, x) \simeq x \left[\frac{1}{9}u_v^p(x) + \frac{4}{9}d_v^p(x) + \frac{10}{9}\bar{u}^p(x) + \frac{2}{9}\bar{s}^p(x) \right] \quad (5.128)$$

and

$$F_2^{ep}(Q^2, x) - F_2^{en}(Q^2, x) \sim \frac{1}{3}x (u_v^p(x) - d_v^p(x)) . \quad (5.129)$$

Integrating over the full x range, one has

$$\int_0^1 \frac{1}{x} \{F_2^{ep}(Q^2, x) - F_2^{en}(Q^2, x)\} dx \simeq \frac{1}{3}. \quad (5.130)$$

This is the so-called Gottfried sum rule. This rule is, however, strongly violated in experimental data (the measured value is 0.235 ± 0.026) showing the limits of the naïve quark–parton model. There is probably an isospin violation in the sea quark distributions.

The Q^2 dependence of the structure functions (Fig. 5.25) was measured systematically by several experiments, in particular, at the HERA electron–proton collider, where a wide Q^2 and x range was covered ($2.7 < Q^2 < 30000 \text{ GeV}^2$; $6 \cdot 10^{-5} < x < 0.65$). For $x > 0.1$, the scaling is reasonably satisfied but for small x , the F_2 structure function clearly increases with Q^2 . This behavior is well predicted by the theory of strong interactions, DGLAP (Dokshitzer–Gribov–Lipatov–Altarelli–Parisi) equations, and basically reflects the resolution power of the exchanged virtual photon. A higher Q^2 corresponds to a smaller wavelength ($\lambda \sim 1/\sqrt{Q^2}$), and therefore a much larger number of sea quarks with a very small x can be seen.

5.5.5 The Number of Quark Colors

A direct experimental test of the number of colors, N_c , comes from the measurement of the R ratio of the hadronic cross section in e^+e^- annihilations to the $\mu^+\mu^-$ cross section, defined as:

$$R = \frac{\sigma(e^+e^- \rightarrow q\bar{q})}{\sigma(e^+e^- \rightarrow \mu^+\mu^-)}. \quad (5.131)$$

At low energies ($\sqrt{s} < m_Z$) these processes are basically electromagnetic and are mediated at the first order by one virtual photon (γ^*). The cross sections are thus proportional to the square of the electric charge q of the final state particles f and \bar{f} . A rule-of-thumb that can frequently be helpful (note the analogies with the Rutherford cross section) above production threshold and outside the regions in which resonances are produced is:

$$\sigma(e^+e^- \rightarrow \mu^+\mu^-) \simeq \frac{4\pi\alpha}{3s} \implies \sigma(e^+e^- \rightarrow f\bar{f}) \simeq \frac{86.8 \text{ nb}}{s/\text{GeV}^2} q^2. \quad (5.132)$$

When considering more than one flavor (for example in the case of hadronic final states), a sum over all the possible final states has to be performed. Thus

$$R = \frac{\sigma(e^+e^- \rightarrow \text{hadrons})}{\sigma(e^+e^- \rightarrow \mu^+\mu^-)} \simeq N_c \sum_i q_i^2. \quad (5.133)$$

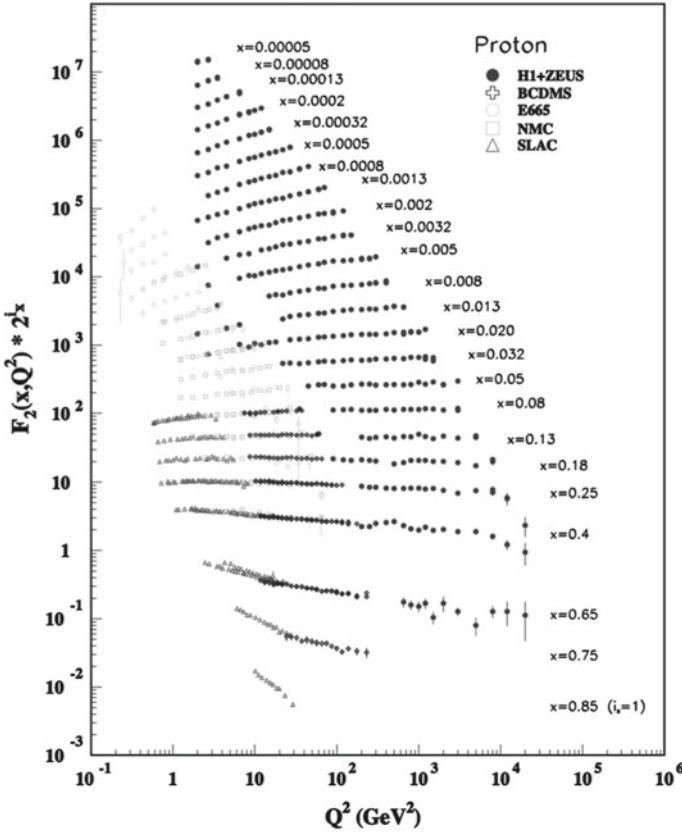


Fig. 5.25 Q^2 dependence of F_2^{ep} . From K.A. Olive et al. (Particle Data Group), Chin. Phys. C 38 (2014) 090001

The sum runs over all the quark flavors with mass $m_i < \frac{1}{2}\sqrt{s}$, and over all colors. For $\sqrt{s} \lesssim 3$ GeV, just the u , d and s quarks can contribute. Then,

$$R = \frac{2}{3} N_c . \tag{5.134}$$

For $3 \text{ GeV} \lesssim \sqrt{s} \lesssim 5 \text{ GeV}$, there is also the contribution of the c quark and

$$R = \frac{10}{9} N_c . \tag{5.135}$$

Finally, for $\sqrt{s} \gtrsim 5 \text{ GeV}$, the b quark contributes

$$R = \frac{11}{9} N_c . \tag{5.136}$$

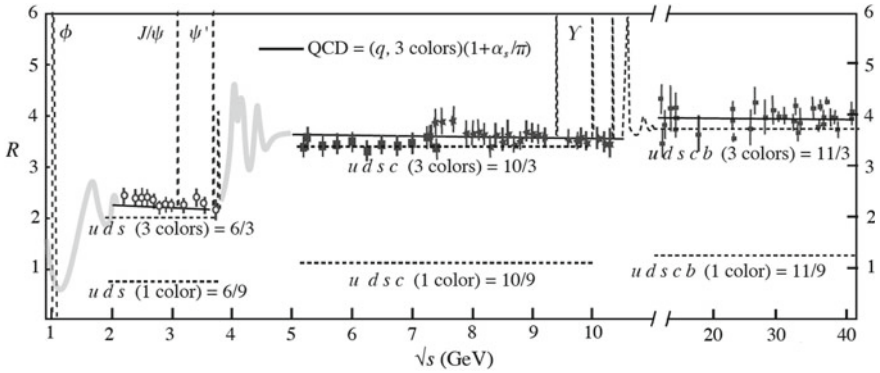


Fig. 5.26 Measurements of $R(\sqrt{s})$. Adapted from [F5.2] in the “further readings”; the data are taken from K.A. Olive et al. (Particle Data Group), Chin. Phys. C 38 (2014) 090001

The mass of the top quark is too high for the $t\bar{t}$ pair production to be accessible at the past and present e^+e^- colliders.

The measurements for $\sqrt{s} \lesssim 40$ GeV, summarized in Fig. 5.26, show, apart from regions close to the resonances, a fair agreement between the data and this naïve predictions, provided $N_c = 3$. Above $\sqrt{s} \gtrsim 40$ GeV, the annihilation via the exchange of a Z boson starts to be nonnegligible and the interference between the two channels is visible, the calculation in Eq. (5.133) being no more valid (see Chap. 7).

5.6 Leptons

The existence of particles not interacting strongly (the leptons) is indispensable to the architecture of the Universe. The first such particle discovered, the electron, has electromagnetic charge -1 and it is one of the fundamental constituents of the atoms. Later on, the neutral neutrino had to be postulated to save the energy-momentum conservation law, as seen in Chap. 2. Finally, three families each made by one charged and one neutral leptons (and their corresponding antiparticles) were discovered, symmetrically with the structure of the three quark families:

$$\begin{pmatrix} \nu_e \\ e^- \end{pmatrix} \begin{pmatrix} \nu_\mu \\ \mu^- \end{pmatrix} \begin{pmatrix} \nu_\tau \\ \tau^- \end{pmatrix}.$$

Electrons, muons, and the experimental proof of the existence of neutrinos were already discussed in Chaps. 2 and 3. Neutrino oscillations and neutrino masses will be discussed in Chap. 9.

The τ (tau) lepton, with its neutrino, was the last discovered.

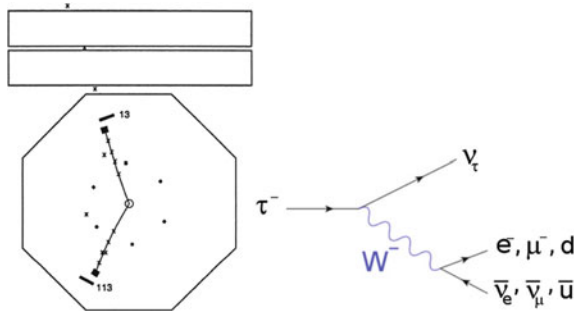


Fig. 5.27 Left: An $e\mu$ event observed at Mark I. The muon moves upward and the electron downward. The numbers 13 and 113 give the relative amount of the electromagnetic energy deposited. Credit: Martin Perl et al., M. L. Perl et al., “Evidence for Anomalous Lepton Production in e^+e^- Annihilation,” *Phys. Rev. Lett.* 35 (1975) 1489. Right: Feynman diagram for the τ^- decay in $\nu_\tau e^- \bar{\nu}_e, \nu_\tau \mu^- \bar{\nu}_\mu, \nu_\tau d \bar{u}$. By en:User: JabberWok and Time 3000 [GFDL <http://www.gnu.org/copyleft/fdl.html>], via Wikimedia Commons

5.6.1 The Discovery of the τ Lepton

The third charged lepton, the τ (tau), was discovered in a series of experiments lead by Martin Perl, using the Mark I detector at the SPEAR e^+e^- storage ring in the years 1974–1976. The first evidence was the observation of events with only two charged particles in the final state: an electron or a positron and an opposite sign muon, with missing energy and momentum (Fig. 5.27, left). The conservation of energy and momentum indicated the existence in such events of at least two undetected particles (neutrinos).

There was no conventional explanation for those events: one had to assume the existence of a new heavy lepton, the τ . In this case, a $\tau^+\tau^-$ pair could have been produced,

$$e^+e^- \rightarrow \tau^+\tau^-$$

followed by the weak decay of each τ into its (anti)neutrino plus a W boson (Fig. 5.27, right); the W boson, as it will be explained in the next chapter, can then decay in one of the known charged leptons ($l = e, \mu$) plus the corresponding neutrino or antineutrino:

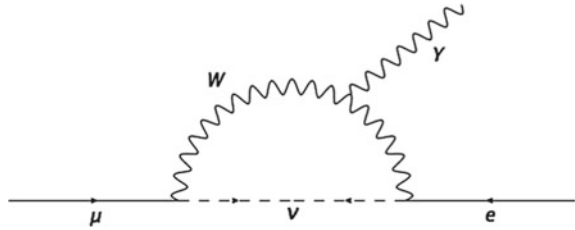
$$\tau^- \rightarrow \nu_\tau W^- \rightarrow \nu_\tau l^- \bar{\nu}_l; \tau^+ \rightarrow \bar{\nu}_\tau W^+ \rightarrow \bar{\nu}_\tau l^+ \nu_l.$$

A confirmation came two years later with the observation of the τ hadronic decay modes:

$$\tau^- \rightarrow \nu_\tau + W^- \rightarrow \nu_\tau + \text{hadrons}.$$

Indeed, the τ is massive enough ($m_\tau \simeq 1.8 \text{ GeV}$) to allow such decays (the W^- being virtual).

Fig. 5.28 Feynman diagram for the decay $\mu^- \rightarrow e^- \gamma$ in the case where just one neutrino species exists



5.6.2 Three Neutrinos

Muons decay into electrons and the electron energy spectrum is continuous. Once again, this excludes a two-body decay and thus at least two neutral “invisible” particles should be present in the final state:

$$\mu^- \rightarrow e^- \nu_1 \bar{\nu}_2.$$

Is $\bar{\nu}_2$ the antiparticle of ν_1 ? Lee and Yang were convinced, in 1960, that it should not be so (otherwise the Feynman diagram represented in Fig. 5.28, would be possible and then the branching fraction for $\mu^- \rightarrow e^- \gamma$ would be large). At least two different species of neutrinos should exist.

Around the same time, the possibility to produce a neutrino beam from the decay of pions created in the collision of GeV protons on a target was intensively discussed in the cafeteria of the Columbia University. In 1962, a kind of a neutrino beam was finally available at Brookhaven National Laboratory (BNL): the idea was to put an internal target in a long straight section of the proton accelerator and to drive with a magnet the proton beam on it; the pions coming from the proton interactions were then decaying into pions. An experiment led by Leon Lederman, Melvin Schwartz, and Jack Steinberger was set to observe the neutrino reaction within a 10-ton spark chamber. Hundreds of millions of neutrinos were produced mostly accompanied by a muon ($BR(\pi \rightarrow \mu\nu) \gg BR(\pi \rightarrow e\nu)$ as it will be discussed in the next chapter). Forty neutrino interactions in the detector were clearly identified; in six of them, the final state was an electron, and in thirty-four, the final state was a muon. The ν_μ and ν_e are, thus, different particles, otherwise the same number of events with one electron and with one muon in the final state should have been observed.

The direct evidence for the third neutrino was established only in the last year of the twentieth century. The DONUT experience at Fermilab found four events in six millions where a τ lepton was clearly identified. In these events, the reconstruction of the charged tracks in the iron/emulsion target showed a characteristic kink indicating at least one invisible particle produced in the decay of a heavy particle into a muon (Fig. 5.29).

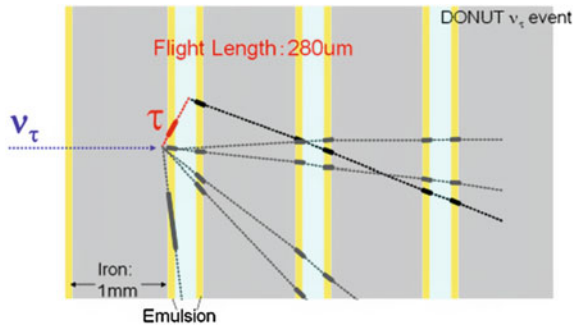


Fig. 5.29 Tau-neutrino event in DONUT. A tau neutrino produces several charged particles. Among them a tau particle, which decays to another charged particle with missing energy (at least one neutrino). From K. Kodama et al., DONUT Collaboration, “Observation of tau-neutrino interactions,” *Phys. Lett. B* 504 (2001) 218

5.7 The Particle Data Group and the Particle Data Book

How can one manage all this information about so many particles? How can one remember all these names? The explosion of particle discoveries has been so great, that Fermi said, “If I could remember the names of all these particles, I’d be a botanist.”

Fortunately, a book, called the Review of Particle Physics (also known as the Particle Data Book), can help us. It is edited by the Particle Data Group (in short PDG), an international collaboration of about 150 particle physicists, helped by some 500 consultants, that compiles and organizes published results related to the properties of particles and fundamental interactions, reviewing in addition theoretical advancements relevant for experimental physics. The PDG publishes the Review of Particle Physics and its pocket version, the Particle Physics Booklet, which are printed biennially in paper, and updated annually in the Web. The PDG also maintains the standard numbering scheme for particles in event generators (Monte Carlo simulations).

The Review of Particle Physics is a voluminous reference work (more than one thousand pages); it is currently the most referenced article in high energy physics, being cited more than 2,000 times per year in the scientific literature. It is divided into three sections:

- Particle physics summary tables—Brief tables with the properties of particles.
- Reviews, tables, and plots—Review of fundamental concepts from mathematics and statistics, tables related to the chemical and physical properties of materials, review of current status in the fields of standard model, cosmology, and experimental methods of particle physics, tables of fundamental physical and astronomical constants, summaries of relevant theoretical subjects.
- Particle listings—Extended version of the Particle Physics Summary Tables, with reference to the experimental measurements.

The Particle Physics Booklet (about 300 pages) is a condensed version of the Review, including the summary tables, and a shortened section of reviews, tables, and plots.

The publication of the Review of Particle Physics in its present form started in 1970; formally, it is a journal publication, appearing in different journals depending on the year.

5.7.1 PDG: Estimates of Physical Quantities

The “particle listings” (from which the “summary tables” are extracted) contain all relevant data known to the PDG team that are published in journals. From these data, “world averages” are calculated.

Sometimes a measurement might be excluded from a world average. Among the reasons of exclusion are the following (as reported by the PDG itself, K.A. Olive et al. (Particle Data Group), *Chin. Phys. C* 38 (2014) 090001):

- it is superseded by or included in later results.
- no error is given.
- it involves questionable assumptions.
- it has a poor signal-to-noise ratio, low statistical significance, or is otherwise of poorer quality than other data available.
- it is clearly inconsistent with other results that appear to be more reliable.

Several kinds of “world average” are provided:

- OUR AVERAGE—From a weighted average of selected data.
- OUR FIT—From a constrained or overdetermined multiparameter fit of data.
- OUR EVALUATION—Not from a direct measurement, but evaluated from measurements of related quantities.
- OUR ESTIMATE—Based on the observed range of the data, not from a formal statistical procedure.

5.7.2 Averaging Procedures by the PDG

The average is computed by a χ^2 minimization. There is an attempt to use uncorrelated variables as much as possible, but correlations are taken into account.

When the error for a measurement x is asymmetric, the error used is a continuous function of the errors δx_+ and δx_- . When the resultant average x is less than $x - \delta x_-$, δx_- is used; when it is greater than $x + \delta x_+$, δx_+ is used; in between, the error is a linear function of x .

Sometimes measurements are inconsistent. Possible inconsistencies are evaluated on the basis of the χ^2 , as follows. The PDG calculates a weighted average and error as

$$\bar{x} \pm \delta\bar{x} = \frac{\sum_i w_i x_i}{\sum_i w_i} \quad \text{with} \quad w_i = \frac{1}{(\delta x_i)^2}. \quad (5.137)$$

Then $\chi^2 = \sum_i w_i (x_i - \bar{x})^2$.

- If $\chi^2/(N - 1)$ is less than or equal to 1, and there are no known problems with the data, the results are accepted.
- If $\chi^2/(N - 1)$ is very large, the PDG may
 - not to use the average at all, or
 - quote the calculated average, making an educated (conservative) guess of the error.
- If $\chi^2/(N - 1)$ is greater than 1, but not so much, the PDG still averages the data, but then also increases the error by $S = \sqrt{\chi^2/(N - 1)}$. This scaling procedure for errors does not affect central values.

If the number of experiments is at least three, and $\chi^2/(N - 1)$ is greater than 1.25, an ideogram of the data is shown in the Particle Listings. Figure 5.30 is an example. Each measurement is shown as a Gaussian with a central value x_i , error δx_i , and area proportional to $1/\delta x_i$.

A short summary of particle properties is also listed in the Appendix D of this book.

Further Reading

- [F5.1] S. Haywood, “Symmetries and Conservation laws in Particle Physics: an introduction to group theory for experimental physicists,” Imperial College Press 2011. An excellent introduction to group theory and its application in particle physics.
- [F5.2] A. Bettini, “Introduction to Elementary Particle Physics,” Cambridge University Press 2014. A very good introduction to Particle Physics at the undergraduate level putting together experimental and theoretical aspects and discussing basic and relevant experiments.
- [F5.3] M. Thomson, “Modern Particle Physics,” Cambridge University Press, 2013. A recent, pedagogical and rigorous book covering the main aspects of Particle Physics at advanced undergraduate and early graduate level.
- [F5.4] PDG 2017, C. Patrignani et al. (Particle Data Group), Chin. Phys. C, 40, 100001 (2016) and 2017 update. URL: <http://pdg.lbl.gov/>. Including the previous editions, this is the most quoted reference in this book.

Exercises

1. *Kinematic thresholds and conservation laws.* Compute the kinematic threshold of the reaction $pp \rightarrow ppp\bar{p}$ in a fixed target experiment.
2. *Can neutron be a bound state of electron and proton?* The hypothesis that the neutron is a bound state of electron and proton is inconsistent with Heisenberg’s uncertainty principle. Why?

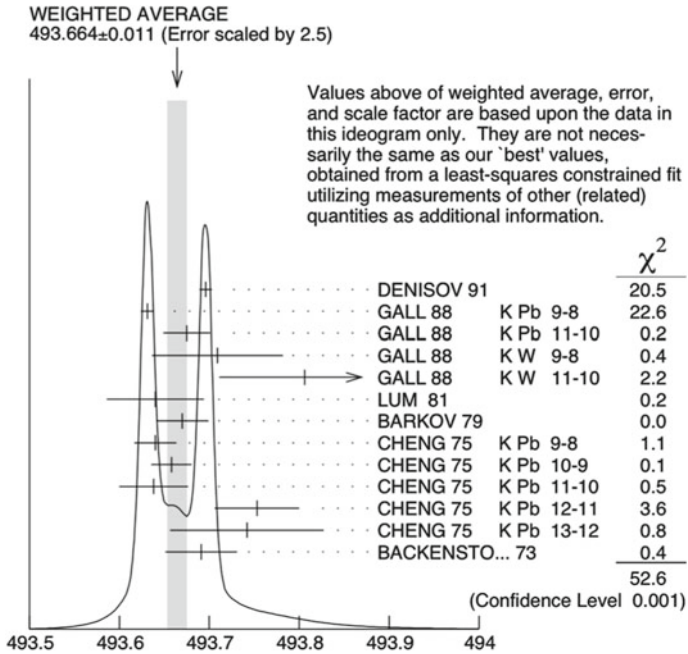


Fig. 5.30 An ideogram representing clearly inconsistent data—the measurements of the mass of the charged kaon. The arrow at the top shows the position of the weighted average, while the width of the shaded pattern shows the error in the average after scaling by the factor S . From K.A. Olive et al. (Particle Data Group), Chin. Phys. C 38 (2014) 090001

3. *Commutation relations.* Demonstrate that if \hat{A} and \hat{B} are two operators the relation (5.42) holds:

$$\exp(\hat{A} + \hat{B}) = \exp\left(\frac{1}{2} [\hat{A}, \hat{B}]\right) \exp(\hat{A}) \exp(\hat{B}).$$

4. *Parity.* Verify explicitly if the spherical harmonics

$$Y_1^{-1}(\theta, \varphi) = \frac{1}{2} \sqrt{\frac{3}{2\pi}} e^{-i\varphi} \sin \theta$$

$$Y_1^0(\theta, \varphi) = \frac{1}{2} \sqrt{\frac{3}{\pi}} \cos \theta$$

$$Y_1^1(\theta, \varphi) = \frac{1}{2} \sqrt{\frac{3}{2\pi}} e^{i\varphi} \sin \theta$$

are eigenstates of the parity operator, and in case they are determine the corresponding eigenvalues.

5. *Constructing baryons.* How many different baryon combinations can you make with 1, 2, 3, 4, 5, or 6 different quark flavors? What's the general formula for n flavors?
6. *Baryons.* Using four quarks ($u, d, s,$ and c), construct a table of all the possible baryon species. How many combinations carry a charm of +1? How many carry charm +2, and +3?
7. *Compositeness of quarks?* M. Shupe [Phys. Lett. B 611, 87 (1979)] has proposed that all quarks and leptons are composed of two even more elementary constituents: c (with charge $-1/3$) and n (with charge zero) - and their respective antiparticles. You are allowed to combine them in groups of three particles or three antiparticles (ccn , for example, or nnn). Construct all of the eight quarks and leptons in the first generation in this manner. (The other generations are supposed to be excited states.) Notice that each of the quark states admits three possible permutations (ccn, cnc, ncc , for example)—these correspond to the three colors.
8. *Decays of the Ξ baryon.* Which decay do you think would be more likely:

$$\Xi^- \rightarrow \Lambda \pi^+ ; \Xi^- \rightarrow n \pi^- .$$

Draw the Feynman diagrams at leading order, and explain your answer.

9. *Decay of charmed mesons.* Which decay do you think would be least likely:

$$D^0 \rightarrow K^- \pi^+ ; D^0 \rightarrow \pi^- \pi^+ ; D^0 \rightarrow \pi^- K^+ .$$

Draw the Feynman diagrams at leading order, and explain your answer.

10. *Cross sections and isospin.* Determine the ratio of the following interactions cross sections at the Δ^{++} resonance: $\pi^- p \rightarrow K^0 \Sigma^0$; $\pi^- p \rightarrow K^+ \Sigma^-$; $\pi^+ p \rightarrow K^+ \Sigma^+$.
11. *Decay branching ratios and isospin.* Consider the decays of the Σ^{*0} into $\Sigma^+ \pi^-$, $\Sigma^0 \pi^0$ and $\Sigma^- \pi^+$. Determine the ratios between the decay rates in these decay channels.
12. *Quantum numbers.* Verify if the following reactions/decays are possible and if not say why:
 - (a) $pp \rightarrow \pi^+ \pi^- \pi^0$,
 - (b) $pp \rightarrow ppn$,
 - (c) $pp \rightarrow ppp\bar{p}$,
 - (d) $p\bar{p} \rightarrow \gamma$,
 - (e) $\pi^- p \rightarrow K^0 \Lambda$,
 - (f) $n \rightarrow pe^- \nu$,
 - (g) $\Lambda \rightarrow \pi^- p$,
 - (h) $e^- \rightarrow \nu_e \gamma$.
13. *Width and lifetime of the J/ψ .* The width of the J/ψ meson is $\simeq 93$ keV. What is its lifetime? Could you imagine an experiment to measure it directly?

14. Ω^- mass. Verify the relations between the masses of all the particles lying in the fundamental baryon decuplet but the Ω^- and predict the mass of this one. Compare your prediction with the measured values.
15. *Decays and conservation laws.* Is the decay $\pi^0 \rightarrow \gamma\gamma\gamma$ possible?
16. *Experimental resolution in deep inelastic scattering.* Consider an e^-p deep inelastic scattering experiment where the electron scattering angle is $\sim 6^\circ$. Make an estimation of the experimental resolution in the measurement of the energy of the scattered electron that is needed to distinguish the elastic channel ($e^-p \rightarrow e^-p$) from the first inelastic channel ($e^-p \rightarrow e^-p\pi^0$).
17. *e^-p deep inelastic scattering kinematics.* Consider the e^-p deep inelastic scattering and deduce the following formulae:

$$Q^2 = 4EE' \sin^2(\theta/2)$$

$$Q^2 = 2M\nu$$

$$Q^2 = xy(s^2 - y^2).$$

18. *Gottfried sum rule.* Deduce in the framework of the quark-parton model the Gottfried sum rule

$$\int \frac{1}{x} (F_2^{ep}(x) - F_2^{ep}(x)) dx = \frac{1}{3} + \frac{2}{3} \int (\bar{u}(x) - \bar{d}(x)) dx$$

and comment the fact that the value measured in e^-p and e^-d deep inelastic scattering experiments is approximately 1/4.